

1 **Moisture damage assessment using surface energy, bitumen stripping**
2 **and the SATS moisture conditioning procedure**

3

4 James Grenfell, Alex Apeageyi and Gordon Airey

5

6 Nottingham Transportation Engineering Centre, University of Nottingham,

7 Nottingham NG7 2RD, United Kingdom.

8 Telephone: +44 115 9513905, Fax: +44 115 9513909

9 Email: james.grenfell@nottingham.ac.uk

10

11 **Abstract**

12

13 Durability is one of the most important properties of an asphalt mixture. A key factor
14 affecting the durability of asphalt pavements is moisture damage. Moisture damage
15 generally results in the loss of strength of the mixture due to two main mechanisms;
16 the loss of adhesion between bitumen and aggregate and the loss of cohesion within
17 the mixture. Conventional test methods for evaluating moisture damage include tests
18 conducted on loose bitumen-coated aggregates and those conducted on compacted
19 asphalt mixtures. The former test methods are simpler and less expensive to conduct
20 but are qualitative/subjective in nature and do not consider cohesive failure while the
21 latter, though more quantitative, are based on bulky mechanical test set-ups and
22 therefore require expensive equipment. Both test methods are, however, empirical in
23 nature thus requiring extensive experience to interpret/use their results. The rolling
24 bottle test (EN 12697-11) for loose aggregate mixtures and the Saturation Ageing
25 Tensile Stiffness (SATS) test (EN 12697-45) for compacted asphalt mixtures are two
26 such methods, which experience suggests, could clearly discriminate between ‘good’
27 and ‘poor’ performing mixtures in the laboratory. A more fundamental approach
28 based on surface energy (SE) measurements offers promise to better understand
29 moisture damage. This paper looks at results from the rolling bottle and the SATS
30 tests in an attempt to better understand the underlying processes and mechanisms of
31 moisture damage with the help of surface energy measurements on the constituent
32 bitumen and aggregates. For this work, a set of bitumens and typical acidic and basic
33 aggregate types (granite and limestone) were selected. Combinations of these

34 materials were assessed using both the rolling bottle and SATS tests. The surface
35 energy properties of the binders were measured using a Dynamic Contact Angle
36 (DCA) Analyser and those of the aggregates using a Dynamic Vapour Sorption
37 (DVS) device. From these surface energy measurements it was possible to predict the
38 relative performance of both the simple rolling bottle test and the more complicated
39 SATS test. Mineralogical composition of the aggregates determined using a Mineral
40 Liberation Analyser (MLA) was used to explain the differences in performance of the
41 mixtures considered.

42

43 Keywords: Bitumen; Asphalt mixtures; Surface energy; Moisture damage; SATS;
44 Rolling Bottle Test, Adhesion, Mineralogical composition.

45

46

47

48

49

50

51

52

53

54

55

56

57

58

59

60

61

62

63

64

65

66

67

68 **1. Introduction**

69

70 The road network is one of the most important elements of a modern transportation
71 system with the majority of roads throughout the world being constructed from
72 asphalt mixtures. Across the United Kingdom, the total budget spent on road
73 maintenance during 2009/10 was of the order of £3.8 billion with moisture damage
74 considered to be one of the major causes of distress in asphalt pavements (Alarm,
75 2010; Audit Scotland, 2010). Although not all damage is caused directly by moisture,
76 its presence increases the extent and severity of already existing distresses like
77 cracking, potholes and rutting (Kennedy et al., 1983; Miller and Bellinger, 2003). The
78 presence of moisture results in the degradation of the mechanical properties of the
79 asphalt mixture, i.e. loss of stiffness and mechanical strength, which ultimately leads
80 to the failure of the road structure. Moisture damage thus has a great economic impact
81 as it causes premature pavement failure and hence results in increased rehabilitation
82 activities and maintenance costs.

83

84 The physical and chemical properties of the two main constituents of an asphalt
85 mixture (bitumen and aggregate) have a direct influence on the moisture performance
86 of the mixture. A lack of compatibility between bitumen and aggregate is one of the
87 main reasons for distress with moisture damage normally being related to the loss of
88 adhesion between bitumen and aggregate and/or loss of cohesion within the bitumen
89 (or more realistically the bitumen-filler mastic) in the presence of water (Terrel and
90 Al-Swailmi, 1994). Removal of bitumen film from the aggregate surface by water is
91 known as ‘stripping’ with this phenomenon depending largely on the chemical
92 composition of the bitumen and aggregates, and their affinity towards each other
93 (Kandhal, 1994; Emery and Seddik, 1997). Previous studies have indicated that the
94 susceptibility of asphalt mixtures to moisture attack is related to bitumen chemistry,
95 aggregate mineralogy, surface texture of the aggregate and the adhesion between the
96 bitumen and aggregates (Airey et al., 2008; Abo-Qudais and Al-Shweily, 2007;
97 Horgnies et al., 2011; Petersen et al., 1982). In addition, the ambient conditions
98 (including temperature, freeze–thaw cycles and wetting–drying cycles) can also
99 significantly affect the durability of an asphalt pavement material (Huang et al., 2005;
100 Gilmore et al., 1985).

101

102 Numerous laboratory test methods have been developed over the years to determine
103 the moisture susceptibility of asphalt mixtures and their response to moisture ingress
104 (Airey and Choi, 2002; Solaimanian et al., 2003). These methods can be divided into
105 two groups: (i) qualitative tests conducted on loose bitumen-coated aggregate, such as
106 the boiling test (Kennedy et al., 1984), and (ii) quantitative tests conducted on
107 compacted asphalt mixtures, such as the wheel tracking test (Aschenbrener, 1995) and
108 the Saturation Ageing Tensile Stiffness (SATS) test procedure (Collop et al., 2004a;
109 Collop et al., 2004a; Airey et al., 2005). The relevant test specimens are typically
110 conditioned in water to simulate in-service conditions and an assessment of any
111 moisture induced damage is made by dividing the conditioned modulus or strength by
112 the corresponding unconditioned property, for example as in the freeze–thaw
113 AASHTO T283-99 procedure (Anon, 2000). In addition to these laboratory test
114 methods, a number of computational approaches have been developed to simulate the
115 in-service conditions experienced by asphalt pavement materials, and hence to attempt
116 to predict the durability and moisture resistance of such materials (Caro et al., 2008a;
117 Caro et al., 2008b; Caro et al., 2010; Masad et al., 2007; Kutay et al., 2007; Shakiba et
118 al., 2013).

119
120 Although these various approaches are realistic and logical in terms of simulating in-
121 service asphalt pavement materials, they do not necessarily attempt to understand in
122 detail the adhesion between bitumen and aggregates, and how such interactions are
123 affected by the presence of moisture and other external factors. It is these physico-
124 chemical properties, directly related to the adhesion characteristics of the two
125 materials, that are responsible for adhesion or debonding between the materials (MS-
126 24, 2007; Kennedy et al., 1982). Surface energy (or more correctly surface free energy
127 (SFE)) properties of the materials can be used to assess these adhesion characteristics
128 (Bhasin, 2006). SFE and various thermodynamic calculations can therefore be
129 successfully used to assess the cohesive and adhesive bond strengths of the two
130 materials and the effect of moisture/water on the bond strength of a bitumen-
131 aggregate system (Bhasin et al., 2006; Cheng et al., 2002a; Cheng et al., 2002b). SFE
132 can therefore be considered to truly represent the physico-chemical surface
133 characteristics of bitumen and aggregates and has been successfully used as a tool for
134 selection of moisture resistant materials (Cheng, 2002). The physico-chemical
135 characteristics of bitumen and aggregates, which can be assessed using surface energy

136 principles, are believed to be a key factor responsible for the adhesion between the
137 two materials.

138

139 This paper presents a framework of surface energy testing techniques with bitumen-
140 aggregate stripping and asphalt mixture mechanical moisture sensitivity assessment
141 for identification of compatible bitumen-aggregate combinations. A complete
142 characterisation is possible once results from SFE measurements and intrinsic
143 adhesion calculations are compared with those of standard mechanical moisture
144 damage tests. Tests like the rolling bottle test (RBT) and the saturated ageing tensile
145 stiffness (SATS) test have been used together with intrinsic adhesion and energy
146 ratios to determine if the moisture sensitivity assessment parameters for different
147 bitumen-aggregate combinations can identify ‘good’ and ‘poor’ performing asphalt
148 mixtures and to determine how the surface energy-based predictions compare with
149 conventional moisture damage test methods.

150

151 **2. Intrinsic adhesion**

152

153 **2.1 Surface free energy theory**

154

155 The surface free energy (SFE) of a material is defined as the energy needed to create a
156 new unit surface area of the material in a vacuum condition. The surface energies of
157 bitumen and aggregate or a bitumen-aggregate system (asphalt mixture) are mainly
158 comprised of an apolar (nonpolar) component and an acid-base component (Fowkes,
159 1962; Good and van Oss, 1991 and Good, 1992). Equation 1 is used to describe the
160 total surface energy and its components:

161

$$162 \quad \gamma = \gamma^{LW} + \gamma^{AB} \quad (1)$$

163

164 Where: γ = surface energy of bitumen or aggregate (mJ/m²);

165 γ^{LW} = Lifshitz–van der Waals component of the surface energy (mJ/m²); and

166 γ^{AB} = acid-base component of the surface energy (mJ/m²).

167

168 The Lifshitz-van der Waals force contains at least three components: London
169 dispersion forces, Debye induction forces, and Keesom orientation forces (Maugis,
170 1999). The acid-base interaction includes all interactions of electron donor (proton
171 acceptor) - electron acceptor (proton donor) type bonds including hydrogen bonding.
172 To quantitatively predict and treat the acid-base interaction, Good and van Oss (1991)
173 postulated a resolution of the acid-base term, γ^{AB} into a Lewis acidic surface
174 parameter and a Lewis basic surface parameter. The relationship among the γ^{AB} and
175 its components is shown in equation 2:

$$177 \quad \gamma^{AB} = 2\sqrt{\gamma^+ \gamma^-} \quad (2)$$

178
179 Where: γ^+ = Lewis acid component of surface interaction, and
180 γ^- = Lewis base component of surface interaction.

181

182 **2.2 SFE measurements**

183

184 Five bitumens were included in the study consisting of four conventional bitumens
185 and one modified bitumen. The conventional bitumens ranged from very hard
186 consistency (10/20 penetration grade) to very soft (160/220 pen grade) with
187 intermediate grades of 40/60 pen and 70/100 pen. The modified bitumen was
188 produced by mixing the 40/60 pen bitumen with an amine-based anti-stripping agent
189 at 0.5% additive by weight of binder. Surface energy components of the five bitumens
190 used in this study were determined indirectly using contact angle measurements.

191

192 A Cahn Model dynamic contact angle (DCA) analyser was used to measure the
193 contact angles of a set of three carefully selected probe liquids on bitumen coated
194 glass slides under dynamic conditions. The probe liquids used included water,
195 glycerol and diiodomethane. All the tests were conducted at room temperature (23°C
196 $\pm 2^\circ\text{C}$) and $50\% \pm 5\%$ relative humidity.

197

198 During the test, a clean 40 mm x 24 mm x 0.45 mm No. 15 microscope glass slide
199 was coated with bitumen and hung from the balance of the DCA equipment with the
200 help of a crocodile clip. A beaker containing a probe liquid was placed on a movable

201 stage positioned under the glass slide. The bottom edge of the slide was kept parallel
 202 with the surface of the probe liquid. The bitumen-coated glass slide was then
 203 immersed up to a maximum depth of 5 mm (advancing) and then withdrawn
 204 (receding) from the liquid by moving the stage up and down, respectively, at a
 205 constant speed of 40 microns/sec while continuously recording the change in mass of
 206 the bitumen-coated slide with depth of immersion. The measured mass-depth
 207 relationships were used to estimate the force acting on the bitumen-slide while being
 208 immersed or removed from probe liquid and used subsequently to determine the
 209 contact angle between bitumen and probe liquid.

210

211 The contact angle (θ) values are obtained by considering the equilibrium forces acting
 212 on the bitumen-coated slide while advancing and receding from the probe liquid using
 213 Eq. 3 (Bhasin, 2006):

214

$$215 \quad \cos \theta = \frac{\Delta F + V_{im}(\rho_L - \rho_{air}g)}{P_t \gamma_L} \quad (3)$$

216

217 Where: P_t = perimeter of the bitumen coated plate

218 γ_L = total surface energy of the probe liquid

219 ΔF = difference between weight of plate in air and partially submerged in
 220 probe liquid

221 V_{im} = volume of solid immersed in the liquid

222 ρ_L = density of the liquid

223 ρ_{air} = air density

224 g = gravitational force

225

226 To obtain surface energy values for the bitumen, contact angle values for at least three
 227 probe liquids are measured and applied to the Young-Dupré equation (Eq. 4) for the
 228 work of adhesion (W_{SL}) between the two materials. Three equations are thus produced
 229 using the known surface energy components of the three probe liquids for the
 230 determination of the three surface energy components ($\gamma^{LW}, \gamma^+, \gamma^-$) of the bitumen.

231

232
$$W_{SL} = \gamma_L (1 + \cos \theta) = 2\sqrt{\gamma_S^{LW} \gamma_L^{LW}} + 2\sqrt{\gamma_S^- \gamma_L^+} + 2\sqrt{\gamma_S^+ \gamma_L^-} \quad (4)$$

233

234 Where subscripts L and S represents liquid and solid respectively, and θ is the contact
 235 angle.

236

237 The resulting surface energy components for the five binders are presented in Table 1.

238 The results for the 70/100 pen bitumen exhibited comparatively lower total surface
 239 energy (19.1 mJ/m²) compared to the results for the 40/60 pen and 10/20 pen
 240 bitumens. However, in general all the results, including the anti-stripping modified
 241 binder (AAS1), are very similar.

242

243 Table 1. Surface energy characteristics of bitumen.

Bitumen	Surface energy components (mJ/m ²)			
	γ^{LW}	γ^+	γ^-	γ
10/20 pen	31.1	0.01	3.37	31.5
40/60 pen	30.6	0.00	2.40	30.6
70/100 pen	19.1	0.00	0.78	19.1
160/220 pen	28.2	0.00	0.30	28.8
AAS1	30.9	0.00	1.00	30.9

244

245 It is difficult to use the contact angle technique on high surface energy materials like
 246 aggregates (SFE values generally > 60 mJ/m²) as probe liquids readily spread on high
 247 energy surfaces and it is difficult to obtain accurate contact angles. Therefore, for this
 248 part of the study a dynamic vapour sorption system (DVS Advantage 2, Surface
 249 Measurement Systems, Middlesex, UK) was used to determine sorption isotherms for
 250 the various aggregates and probe vapour combinations and the results used to
 251 determine the SFE components of the aggregate. The desired partial vapour pressures
 252 were varied from 0 to 95% with 5-10% increments (14 steps).

253

254 Five aggregates commonly used in UK asphalt mixtures were chosen for the study.
 255 The aggregates (two ‘limestones’ and three ‘granites’) were selected based on their
 256 difference in mineralogy and the fact that they exhibit different moisture damage
 257 performance (Airey et al., 2007). The mineralogy of the different aggregates was
 258 studied using a Mineral Liberation Analyser (MLA) in order to understand their
 259 morphology and to help with the overall analysis of results.

260

261 MLA comprises a procedure used to identify the mineral phases present in aggregates
 262 by combining a large specimen chamber automated Scanning Electron Microscope
 263 (SEM) and multiple Energy Dispersive X-ray detectors with automated quantitative
 264 mineralogy software. The software controls the SEM hardware to quantitatively
 265 analyse mineral and material samples. Automated stage control and image acquisition
 266 allows for rapid and systematic Back Scattered Electron (BSE) imaging and
 267 subsequent X-ray analysis of thousands of mineral grains and particles. Automatic
 268 recalibration ensures consistent results.

269

270 An FEI Quanta 600 SEM with MLA capability was used for the mineral phase
 271 determination. Aggregate samples were prepared by casting aggregates in resin,
 272 followed by polishing of the surface. The samples were then carbon coated to make
 273 them electron conductive and scanned in BSE mode with Electron Dispersive X-ray
 274 analysis (EDX) being carried out in an array of spots across the particles. The
 275 resultant spectra were then used to determine mineral phases at specific points in the
 276 microstructure which allowed mineralogical maps to be generated for each of the
 277 aggregate types (Grenfell et al., 2014).

278

279 Table 2. Mineral composition of aggregates obtained using MLA.

Mineral name	Composition (%)		
	Granite A	Granite B	Granite C
Quartz	19.11	15.86	33.17
Albite	27.13	32.73	28.30
K-feldspar	4.82	9.64	16.93
Chlorite	31.53	13.52	11.90
Muscovite	2.39	3.43	4.58
Other	0.74	1.91	1.19
Epidote	11.11	1.37	1.06
Biotite	0.99	0.34	1.00
Anorthite	0.10	18.54	0.82
Calcite	0.20	0.08	0.78
Hornblende	1.88	2.57	0.27
	Limestone A	Limestone B	
Calcite	96.98	98.94	
Dolomite	1.30	0.00	
Clay	0.93	0.37	
Quartz	0.49	0.55	
Other	0.30	0.13	

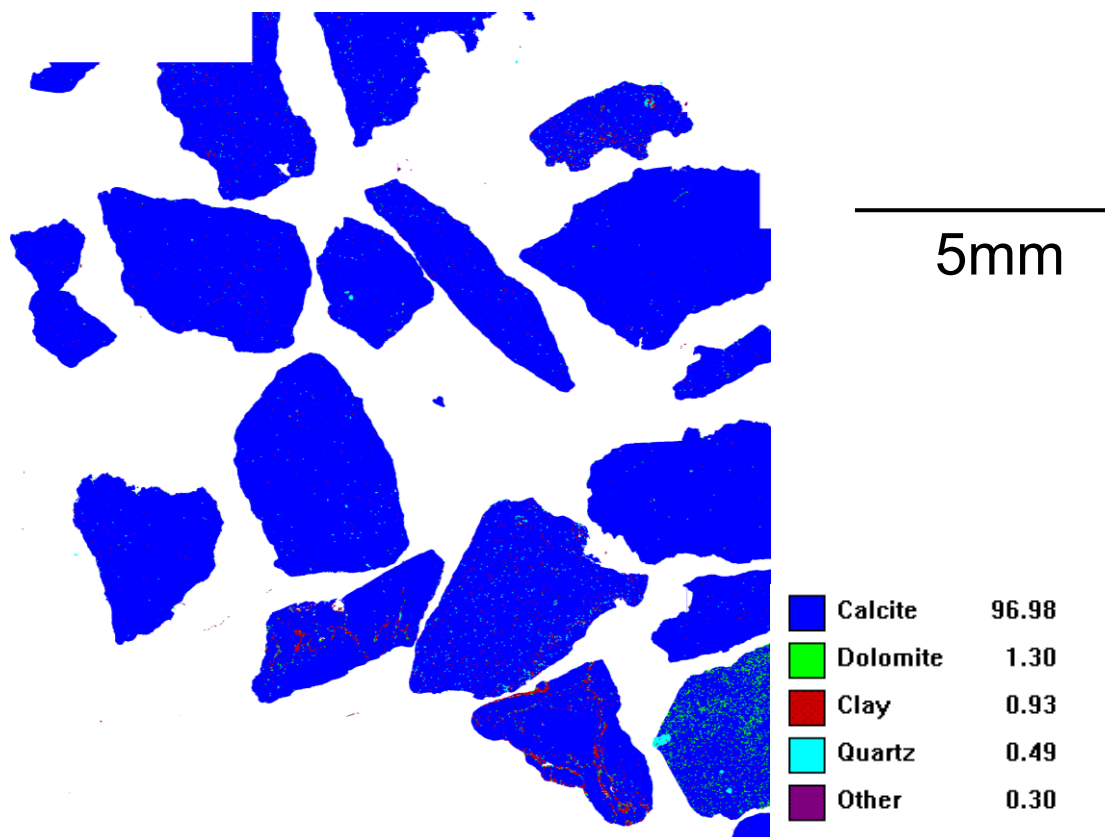
280 K-feldspar = potassium-dominant feldspar

281

282 The MLA results (in terms of mineral composition) for the five aggregates are
 283 presented in Table 2 and examples of the MLA scans for two of the aggregates

284 (Limestone A and Granite A) are presented in Figures 1 and 2. The results show that
285 the aggregates have significantly different mineralogical make-up with Limestone A
286 (Figure 1) being made up of predominantly (about 97%) calcite. Granite C, on the
287 other hand, is made up of a number of different mineral phases with the predominant
288 phase being quartz, but with significant quantities of albite and K_feldspar (see Figure
289 2). It is believed that the large proportion of the quartz phase has the potential to lead
290 to deleterious moisture properties, due to the poor adhesion between quartz and
291 bitumen. However, there is also evidence that high feldspar content can be responsible
292 for interfacial failure between bitumen and aggregate surfaces (Horgnies et al., 2011).
293

294 In general, the limestone aggregates, being basic, are believed to perform better in
295 practice as well as in moisture sensitivity tests, while the granite aggregates have been
296 found to perform poorly in previous moisture sensitivity work (Grenfell et al., 2012).
297
298

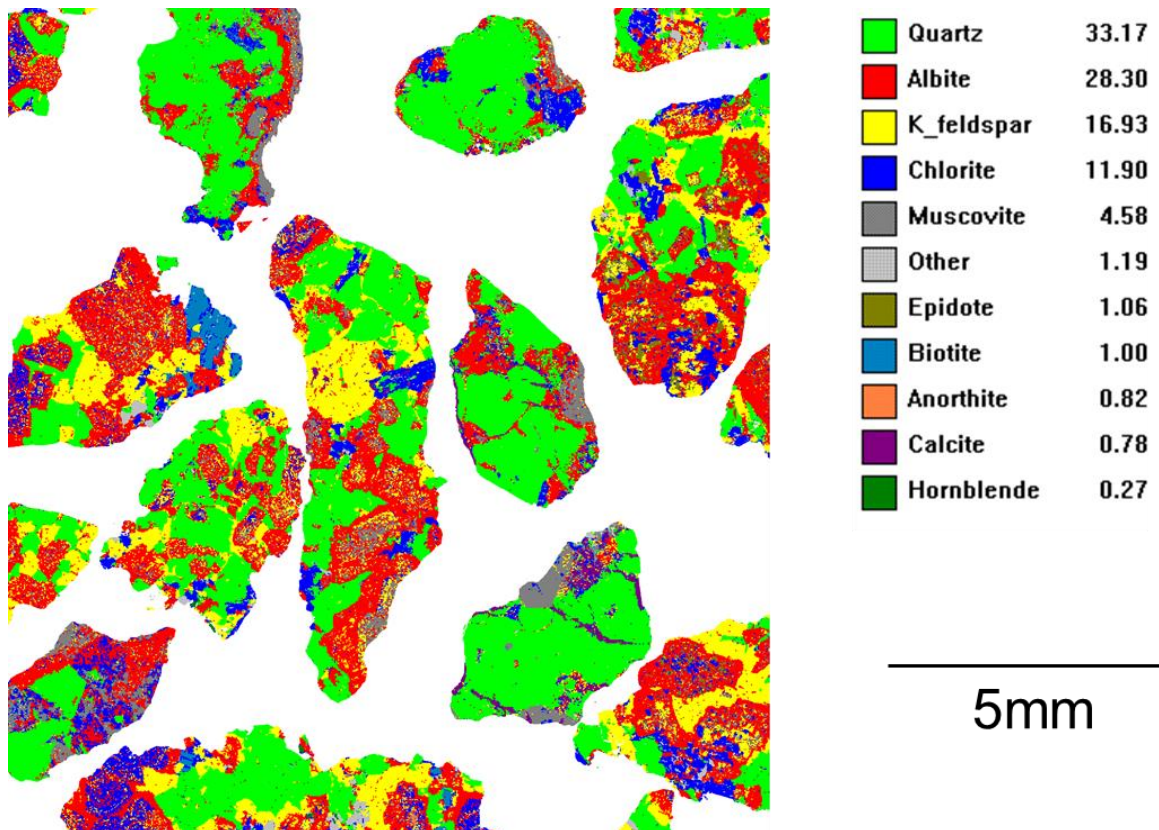


299
300
301
302

Figure 1. MLA analysis of Limestone A.

303 Prior to surface energy testing, the aggregates were first washed with deionised water
 304 and then dried in an oven to constant mass (up to 16 hours). An aggregate fraction
 305 passing 5mm and retained on 2.36mm was used. The upper limit on aggregate size is
 306 dictated by the material holding capacity of the DVS sample chamber. The cleaned
 307 oven-dried aggregate samples (less than 10 g) were again pre-heated in the DVS
 308 sample chamber at a temperature of 110°C for up to five hours to completely dry the
 309 samples before the sorption test.

310



311

312

313 Figure 2. MLA analysis of Granite C.

314

315 To perform the sorption test, carefully selected probe vapours (octane, ethyl acetate,
 316 and chloroform) with known SFE components were passed through the aggregate
 317 sample, under controlled temperature and partial vapour pressure conditions, with the
 318 aid of an inert carrier gas (nitrogen). The probes that were chosen for the aggregate
 319 testing had relatively low surface tension values as compared to the ones that are used
 320 for testing the bitumen to aid the ability to achieve a uniform adsorption/monolayer of
 321 the probe on the aggregate surface. Due to the surface characteristics of the aggregate,

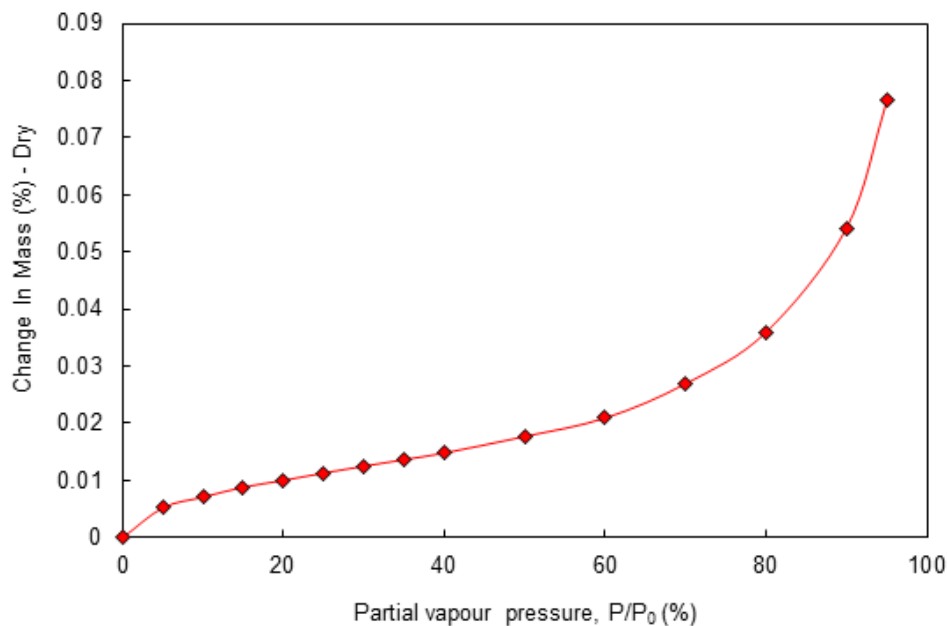
322 vapour probes get adsorbed on their surfaces which results in an increase in the mass
323 of the aggregate sample that is then measured using a sensitive balance.

324

325 During the test, the aggregate material was exposed to different concentrations/vapour
326 pressures of the probe liquids and the increase in mass of the aggregates, because of
327 adsorption of the probe vapours on the aggregate surface, was measured. All the tests
328 were performed at a temperature of 25°C. The change in mass of an aggregate sample
329 was plotted against the increasing partial vapour pressure values to generate sorption
330 isotherms which were used to estimate specific surface area and spreading equilibrium
331 pressures of the aggregates.

332

333 A typical obtained adsorption isotherm is shown in Figure 3 for Limestone A
334 aggregate with octane probe vapour for partial vapour pressures (concentrations)
335 ranging from 0 to 95%. Similar isotherms were obtained for the other aggregates.



336

337 Figure 3. Typical sorption isotherm obtained for Limestone A aggregate using octane
338 vapour as probe for partial vapour pressures (concentration) ranging from 0 to 95%
339 with 5-10% increments (14 steps).

340

341 From Figure 3, it can be seen that the plot of adsorbed mass versus partial vapour
342 pressures for Limestone A shows characteristics typical of Type II isotherms (Erbil,

2006). This suggests that the BET model can be used to fit the sorption isotherms (up to 35% partial vapour pressure) using the Langmuir approach (Eq. 5) where a plot of $P/(P_0-P)n$ against P/P_0 gives a straight line from which the BET constant (c) and the specific amount of vapour adsorbed on the surface of aggregate (n_m), can be obtained. The results were used to estimate the specific surface area of the aggregates using Eq. 6 (Shaw, 1991; Sing, 1969).

349

$$\frac{P}{n(P_0 - P)} = \left(\frac{c - 1}{n_m c} \right) \frac{P}{P_0} + \frac{1}{n_m c} \quad (5)$$

351

Where: P = partial vapour pressure, Pa

P_0 = saturated vapour pressure of solvent, Pa

n = specific amount adsorbed on the surface of the absorbent, mg; and

c = BET constant (parameter theoretically related to the net molar enthalpy of the adsorption)

357

$$SSA = \left(\frac{n_m N_0}{M} \right) \alpha \quad (6)$$

359

Where: SSA = specific surface area of solid, m^2

n_m = monolayer specific amount of vapour adsorbed on the aggregate surface, mg

N_0 = Avogadro's number, $6.022 \times 10^{23} \text{ mol}^{-1}$

M = molecular weight of the vapour, g/mol

α = projected or cross-sectional area of the vapour single molecule, m^2

366

In addition to estimating the specific surface as previously described, the sorption isotherms were also used to calculate the spreading pressure which is required to determine surface energy components of the aggregates. Adsorption of vapour molecules on the aggregate surface reduces its SFE, so spreading pressure, as a result of adsorption of the vapour molecules, can be expressed as:

372

$$\pi_e = \gamma_s - \gamma_{sv} \quad (7)$$

374 Where: π_e = spreading pressure at maximum saturated vapour pressure or equilibrium

375 spreading pressure, mJ/m^2

376 γ_s = aggregate surface energy in vacuum

377 γ_{SV} = aggregate surface energy after exposure to vapour

378

379 Spreading pressure at maximum saturation vapour pressure, π_e , for each solvent is

380 calculated by using the following Gibbs free energy model (Eq. 8):

381

$$382 \quad \pi_e = \frac{RT}{A} \int_0^{P_0} \frac{n}{P} dP \quad (8)$$

383

384 Where: R = universal gas constant, $83.14 \text{ cm}^3 \text{ bar/mol.K}$

385 T = absolute temperature, K

386

387 By introducing spreading pressure, π_e , in the Young-Dupré relation (Eq. 4), the

388 following relationship is obtained:

389

$$390 \quad W_{SL} = \pi_e + \gamma_{LV} (1 + \cos \theta) \quad (9)$$

391

392 The contact angle value for high energy solids such as aggregates is zero, therefore,

393 Eq. 9 can be re-written as:

394

$$395 \quad W_{SL} = \pi_e + 2\gamma_{LV} \quad (10)$$

396

397 By substituting the above relation in Eq. 4, the following equation is obtained:

398

$$399 \quad 2\gamma_L + \pi_e = 2\sqrt{\gamma_S^{LW} \gamma_L^{LW}} + 2\sqrt{\gamma_S^+ \gamma_L^-} + 2\sqrt{\gamma_S^- \gamma_L^+} \quad (11)$$

400

401 From Eq. 11, if the spreading pressures from three different probe vapours are

402 measured, then the three surface energy components of the aggregates ($\gamma_S^{LW}, \gamma_S^+, \gamma_S^-$)

403 can be determined by solving three simultaneous equations.

404 For the five aggregates, only fractions passing the 5 mm sieve and retained on the
 405 2.36 mm sieve were tested and reported in this paper. The results were used to
 406 estimate specific surface area (SSA) and equilibrium pressure from which the surface
 407 energy parameters were calculated.

408

409 Specific surface area obtained for the five aggregates are presented in Table 3 using
 410 octane as the probe vapour. Specific surface area for the various aggregates showed
 411 large differences depending on aggregate type. The differences can be attributed to the
 412 different microstructure of the aggregates. The specific surface area obtained for each
 413 aggregate was used in two different ways: 1) to determine the equilibrium spreading
 414 pressure and 2) to calculate the moisture compatibility ratios.

415

416 Table 3. Surface energy characteristics of aggregates.

Aggregate	Surface energy components (mJ/m ²)				SSA (m ² /g)
	γ^{LW}	γ^+	γ^-	γ	
Limestone A	75.3	108.9	49.7	222.4	0.1708
Limestone B	66.3	2.9	4.9	73.8	0.7863
Granite A	69.1	17.3	568.3	267.4	0.3819
Granite B	68.3	16.4	40.8	120.0	0.3807
Granite C	68.0	163.9	122.7	351.6	0.4420

417

418 The SSA values were used to calculate the equilibrium spreading pressures on the
 419 aggregate surfaces for all three probes. Octane, being non-polar in nature, is supposed
 420 to give more accurate values of surface area (because non-polar substances do not
 421 have affinity for polar substances). The obtained spreading pressures were then used
 422 to compute the surface energy components ($\gamma_s^{LW}, \gamma_s^+, \gamma_s^-$) as well as the total surface
 423 energy (γ_s) for the aggregates as listed in Table 3.

424

425 The results show that surface energy properties vary considerably, in terms of surface
 426 energy components as well as total surface energy, amongst the different aggregates.
 427 The differences can be attributed to different elemental and mineralogical
 428 compositions of the aggregates. The test results indicate that there is not a significant
 429 difference between the van der Waals components of the aggregates (all
 430 approximately 70 mJ/m²) but there are significant differences between the acid-base
 431 components of the limestone and granite aggregates. On the basis of total surface
 432 energy alone, and for the same bitumen, Granite C ($\gamma = 351.6$ mJ/m²) should

433 theoretically form stronger adhesive bond than Limestone B ($\gamma = 73.8 \text{ mJ/m}^2$). Note
434 that this assertion assumes a completely dry aggregate.

435

436 2.3 Adhesion calculations

437

438 The surface energy properties of the bitumen and the aggregates on their own have
439 very little significance. However, when combined thermodynamically, they are
440 helpful for estimating the interfacial work of adhesion between the two materials, with
441 or without the presence of moisture.

442

443 The main objective for measuring surface energy of bitumen and aggregates is to be
444 able to estimate the moisture sensitivity of asphalt mixtures using the principles of
445 thermodynamics and physical adhesion. This objective was accomplished by using the
446 surface energy properties of the aggregate and bitumen to calculate their interfacial
447 work of adhesion (dry bond strength) and the reduction in free energy of the system
448 (work of debonding) when water displaces bitumen from the aggregate-bitumen
449 interface (Eqs 12 and 13). For an asphalt mixture to be durable and less sensitive to
450 moisture, it is desirable that the work of adhesion between the bitumen and the
451 aggregate be as high as possible.

452

453 In addition to the two parameters: dry bond strength and work of debonding, a third
454 parameter, the cohesion of bitumen, can be calculated from the surface energy
455 properties of bitumen. These three bond energy parameters (bitumen cohesion, dry
456 bond strength, and work of debonding) can then be used to assess the moisture
457 sensitivity of an asphalt mixture. Bitumen cohesion is the cohesive bond strength of
458 the material and is estimated as twice the total surface energy of the material. Dry
459 bond strength (W_{BA}^a) is defined as given in Eq. 12 as the interfacial work of adhesion
460 between the bitumen (B) and aggregate (A). A higher value of dry bond strength
461 suggests greater adhesion between the two materials and hence more resistance
462 against debonding.

463

$$464 W_{BA}^a = 2\sqrt{\gamma_B^{LW} \gamma_A^{LW}} + 2\sqrt{\gamma_B^+ \gamma_A^-} + 2\sqrt{\gamma_B^- \gamma_A^+} \quad (12)$$

465

466 Eq. 13 gives the work of debonding (W_{BWA}^a) which is considered as the reduction in
 467 bond strength of a bitumen-aggregate system when water (W) is introduced into the
 468 system or when water displaces the bitumen from the aggregate surface. This quantity
 469 might also be interpreted as the energy required for water to separate or break the
 470 bond of bitumen-aggregate systems.

471

472 In general, (W_{BWA}^a) is found to be a negative value for most aggregate-bitumen
 473 systems. This means that the process of water breaking or separating the existing
 474 adhesive aggregate-bitumen bond is a thermodynamically favourable process. In other
 475 words, no external work is required for this separation process to occur once water
 476 reaches the aggregate-bitumen interface. A smaller absolute value of this parameter
 477 for a given bitumen-aggregate system is indicative of a better moisture damage
 478 performance of that system.

479

$$\begin{aligned}
 W_{BWA}^a = & \left\{ \left(\left(\sqrt{\gamma_A^{LW}} - 4.67 \right)^2 \right) + \left(2 \times \left(\sqrt{\gamma_A^+} - 5.05 \right) \times \left(\sqrt{\gamma_A^-} - 5.05 \right) \right) \right\} \\
 480 & + \left\{ \left(\left(\sqrt{\gamma_B^{LW}} - 4.67 \right)^2 \right) + \left(2 \times \left(\sqrt{\gamma_B^+} - 5.05 \right) \times \left(\sqrt{\gamma_B^-} - 5.05 \right) \right) \right\} \\
 & - \left\{ \left(\left(\sqrt{\gamma_B^{LW}} - \sqrt{\gamma_A^{LW}} \right)^2 \right) + \left(2 \times \left(\sqrt{\gamma_B^+} - \sqrt{\gamma_A^+} \right) \times \left(\sqrt{\gamma_B^-} - \sqrt{\gamma_A^-} \right) \right) \right\}
 \end{aligned} \tag{13}$$

481

482 Work of adhesion results for the various aggregate-bitumen combinations are
 483 presented in Table 4. The results show both the influence of the different aggregates
 484 and bitumen on work of adhesion.

485

486 Table 4. Work of adhesion between bitumen and aggregates.

Bitumen	Work of adhesion (mJ/m ²)				
	Limestone A	Limestone B	Granite A	Granite B	Granite C
10/20 pen	136	98	113	108	141
40/60 pen	128	95	105	104	131
70/100 pen	94	74	80	79	95
160/220 pen	104	88	93	92	102
AAS1	117	94	101	100	117

487

488 Work of debonding values for the aggregate-bitumen combinations are presented in

489 Table 5.

490 Table 5. Work of debonding in the presence of water.

Bitumen	Work of debonding (mJ/m ²)				
	Limestone A	Limestone B	Granite A	Granite B	Granite C
10/20 pen	-47	56	-174	-32	-103
40/60 pen	-51	58	-177	-35	-109
70/100 pen	-67	55	-185	-52	-128
160/220 pen	-64	63	-177	-16	-126
AAS1	-57	62	-176	-13	-117

491

492 In addition to the work of adhesion, the greater the magnitude of work of debonding
 493 when water displaces bitumen from the aggregate-bitumen interface (in terms of
 494 absolute values of this quantity), the greater will be the thermodynamic potential that
 495 drives moisture damage. Granite A and Granite C therefore have a far greater
 496 potential for moisture damage compared to the limestone aggregates and Granite B. In
 497 addition, the positive values for Limestone B indicate that external work or energy
 498 would be required for water to be able to separate the existing adhesive bond between
 499 the different binders and this aggregate. In other words, of all the aggregate-bitumen
 500 combinations, those with Limestone B have the greatest potential resistance to
 501 debonding caused by water.

502

503 The results also show that for a given aggregate, work of debonding (absolute values)
 504 generally increases slightly (in magnitude) for softer bitumen compared to harder
 505 (stiffer) binders. This is true for Limestone A and B as well as Granite C although the
 506 results for Granite A are fairly consistent for all four penetration grade bitumens and
 507 there is a considerable decrease in absolute value for the soft 160/220 pen bitumen for
 508 Granite B.

509

510 **2.4 Adhesion bond energy parameters**

511

512 The ratio (ER_1) between the adhesive bond energy values in the dry condition (W_{BA}^a)
 513 and in the presence of water (W_{BWA}^a) can be used to predict the moisture sensitivity of
 514 asphalt mixtures. A higher value of energy ratio indicates better resistance to moisture
 515 damage for that bitumen-aggregate combination. Bhasin et al. (2006) used energy
 516 ratio ER_1 to study different types of asphalt mixtures and concluded that mixtures with
 517 a ratio higher than 1.5 were more moisture resistant than the ones with ratios lower
 518 than 0.8.

$$ER_1 = \left| \frac{W_{BA}^a}{W_{BWA}^a} \right| \quad (14)$$

520

521 Aggregates with higher surface roughness and greater surface area are supposed to
 522 bond better with bitumen by providing more bond area and better interlocking. In
 523 order to accommodate this effect, a second bond energy parameter ($ER_1 \cdot SSA$ or ER_3)
 524 obtained by multiplying the bond energy ratio (ER_1) with specific surface area (SSA)
 525 has been proposed in addition to ER_1 to predict moisture sensitivity of asphalt
 526 mixtures (Bhasin et al., 2006).

527

528 Wetting/coating of an aggregate with bitumen is not only affected by the surface
 529 properties of the two materials; the viscosity or cohesion of the bitumen itself also
 530 plays a very important role. Bitumen with lesser cohesion and greater affinity for the
 531 aggregates will have a higher wettability and will coat the aggregate surface more
 532 than bitumen having lesser wettability characteristics. However, softer bitumen
 533 having lesser cohesion may be more prone to emulsification (decrease in cohesion) in
 534 the presence of water. The effects of cohesion and wettability on moisture resistance
 535 can be accounted for by modifying the ER_1 parameter by replacing the bond strength
 536 in the dry condition (W_{BA}^a) with a wettability relationship ($W_{BA}^a - W_{BB}$). This new
 537 moisture sensitivity assessment parameter (ER_2) is given in Eq. 15 (Bhasin, 2006). In
 538 order to accommodate the effects of aggregate micro-texture on the bitumen-
 539 aggregate bond strength in the presence of moisture, the bond parameter ER_2 can be
 540 multiplied by specific surface area of the aggregates to obtain a fourth bond energy
 541 parameter ($ER_2 \cdot SSA$ or ER_4) (Bhasin, 2006).

542

$$ER_2 = \left| \frac{W_{BA}^a - W_{BB}}{W_{BWA}^a} \right| \quad (15)$$

544

545 Where (W_{BA}^a) and (W_{BB}) represent bitumen-aggregate dry bond strength and bitumen
 546 cohesion respectively.

547

548 These four bitumen-aggregate bond energy parameters (ER_1 , ER_2 , ER_3 and ER_4) were
 549 used to assess the moisture susceptibility of the asphalt mixtures. In all cases, higher

550 energy ratios are associated with mixtures with better moisture resistance. It is
 551 important to note that the energy ratios have been developed for aggregate-binder
 552 systems that demonstrate a negative value for the work of adhesion under ‘wet’
 553 conditions (W_{BWA}^a) and are therefore are not applicable for the systems containing
 554 Limestone B which produced positive values of W_{BWA}^a as shown in Table 5.

555

556 Table 6 shows the aggregate-bitumen bond energy parameters (ER₁, ER₂, ER₃ and
 557 ER₄) for the asphalt mixtures (bitumen-aggregate combinations). Values have been
 558 included for the aggregate-bitumen combinations containing Limestone B although,
 559 as explained above, they do not represent the actual resistance of the mixture to
 560 moisture damage.

561

562 Table 6. Bond energy parameters for aggregate-bitumen combinations.

Bitumen	Limestone A	Limestone B	Granite A	Granite B	Granite C	Threshold criteria ^a
ER ₁						
10/20 pen	2.90	1.74 ^b	0.65	3.41	1.37	≥ 0.75
40/60 pen	2.52	1.64 ^b	0.59	2.93	1.20	
70/100 pen	1.40	1.36 ^b	0.43	1.54	0.74	
160/220 pen	1.63	1.40 ^b	0.52	5.81	0.81	
AAS1	2.07	1.52 ^b	0.57	7.86	1.00	
ER ₂						
10/20 pen	1.56	0.62 ^b	0.29	1.86	0.76	≥ 0.50
40/60 pen	1.32	0.59 ^b	0.25	1.56	0.64	
70/100 pen	0.83	0.66 ^b	0.23	0.94	0.44	
160/220 pen	0.74	0.51 ^b	0.21	2.26	0.36	
AAS1	0.98	0.52 ^b	0.22	3.00	0.47	
ER ₃						
10/20 pen	0.49	1.37 ^b	0.25	1.30	0.61	≥ 0.50
40/60 pen	0.43	1.29 ^b	0.23	1.12	0.53	
70/100 pen	0.24	1.07 ^b	0.17	0.59	0.33	
160/220 pen	0.28	1.10 ^b	0.20	2.21	0.36	
AAS1	0.35	1.19 ^b	0.22	2.99	0.44	
ER ₄						
10/20 pen	0.27	0.49 ^b	0.11	0.71	0.34	≥ 0.35
40/60 pen	0.22	0.46 ^b	0.09	0.59	0.28	
70/100 pen	0.14	0.52 ^b	0.09	0.36	0.20	
160/220 pen	0.13	0.40 ^b	0.08	0.86	0.16	
AAS1	0.17	0.41 ^b	0.08	1.14	0.21	

563 ^aafter Little and Bhasin (2006)

564 ^bComputed but not applicable for moisture damage assessment

565

566 It is worth reiterating that the energy ratios used in this paper and presented in Table 6
567 are based on absolute values. These ratios therefore do not take into account
568 differences in the thermodynamic processes associated with debonding caused by
569 water which means that all four bond energy ratios treat all five aggregates the same.
570 Clearly this is not the case with Limestone B showing a positive value for the work of
571 debonding (W_{BWA}^a) compared to the negative values obtained for the other four
572 aggregates. This implies that all combinations with this aggregate should have higher
573 energy ratios than those reported in Table 6 in order to reflect the greater resistance to
574 debonding in the presence of water. As this has not been done in the paper, it is
575 important to consider the energy ratio results for Limestone B as conservative values.

576

577 The four bond energy parameters can be used to predict the moisture sensitivity of
578 asphalt mixtures using threshold values defined to separate ‘good’ from ‘poor’
579 moisture damage performing aggregate-bitumen combinations. The threshold limits
580 are 0.75 for ER₁, 0.50 for ER₂, 0.50 for ER₃ and 0.35 for ER₄ (Bhasin, 2006; Bhasin
581 et al., 2006; Little and Bhasin, 2006). Once again, the criteria given by Bhasin to
582 differentiate between ‘good’ and ‘poor’ performing mixtures were obtained using data
583 in which all aggregate-binder combinations had negative values of work of adhesion
584 in the presence of water and are therefore are not applicable for any of the
585 combinations with Limestone B.

586

587 In general the limestone aggregate-bitumen combinations tend to have higher values
588 compared to the granite aggregate-bitumen combinations although the values for
589 Granite B, especially ER₁ and ER₂, are very high. The results show that the ranking of
590 the ‘good’ versus ‘poor’ moisture damage performing aggregate-bitumen
591 combinations for ER₁ and ER₂ are quite similar; both parameters placing the same
592 number of combinations in ‘good’ versus ‘poor’ categories. The results for the other
593 two parameters, ER₃ and ER₄, are also similar but the later placed more mixtures in
594 the ‘poor’ category. The results suggest, for the materials considered, that ER₁ and
595 ER₂ are sensitive to binder cohesion as the softer 70/100 pen bitumen showed lower
596 ratios irrespective of the aggregate type. In addition, the use of an anti-stripping
597 additive (binder AAS1) has not appeared to affect the bond energy ratios compared to

598 those found for the 40/60 pen base bitumen with the only exception being the values
599 for Granite B which showed a significant increase.

600

601 Compared to the ER_1 and ER_2 parameters, the results for ER_3 and ER_4 show the
602 significant influence of SSA on the selection of ‘good’ versus ‘poor’ moisture damage
603 performing aggregate-bitumen combinations. Because of the apparent large influence
604 of SSA on moisture sensitivity of asphalt mixtures shown in Table 6, the bond
605 parameters ER_3 and ER_4 appear to be more suitable indices for determining the
606 performance of the different aggregate-bitumen combinations with a clear distinction
607 in terms of ‘good’ and ‘poor’ aggregates.

608

609 **3. Aggregate-bitumen stripping**

610

611 The same five aggregates (two limestones and three granites) and two of the binders
612 (40/60 pen and 160/220 pen) were tested using the four aggregate-bitumen stripping tests.
613 In addition, the anti-stripping modified binder AAS1 was also used with the five
614 aggregates but only for two of the aggregate-bitumen stripping tests due to shortages in
615 the supply of the amine-based anti-stripping agent. Based on field experience, the
616 limestone aggregates tend to be more resistant to moisture damage than the granite
617 aggregates. Therefore, it was expected that a discriminating laboratory test should be able
618 to distinguish between the mixtures based on the selected aggregates.

619

620 In most of the existing test standards for evaluating moisture resistance of loose asphalt
621 mixtures, the most commonly used aggregate sizes range from 6.3 mm to 9.5 mm.
622 Therefore, for each of the five aggregate types selected for testing, only material passing
623 the 9.6 mm sieve size but retained on the 6.3 mm sieve was used.

624

625 **3.1 Static immersion test**

626

627 The static immersion test was conducted in accordance with ASTM D1664 (AASHTO
628 T182). During the test, a 100 g sample of aggregate with sizes ranging from 6.3 to 9.5
629 mm coated with 5.5 g of bitumen was immersed in distilled water at 25°C for 16 to 18
630 hours in a 500 ml glass bottle. The sample was then observed through the glass to
631 estimate the percentage of total visible area of aggregate that remains coated as above or

632 below 95%. Three replicate 100 g aggregate samples coated with bitumen were tested
633 and the average percentage coated estimated. Some of the disadvantages of the test are 1)
634 the test is subjective and therefore has high variability and, 2) the test does not involve
635 any strength tests that directly relate to mixture performance.

636

637 The results in terms of percentage of total visible area of aggregate that remains coated
638 after 16 to 18 hours of soaking are presented in Figure 4. The results indicated that 100%
639 of the aggregate remained coated at the end of the test for all the limestone aggregate
640 mixtures. For the granite mixtures, the percentage coated area observed for each
641 aggregate was above 95% with the exception of Granite C that showed about 90% coated
642 area.

643

644

645

646

647

648

649

650

651

652

653

654

655

656

657

658

659

660

661

662

663

664

665

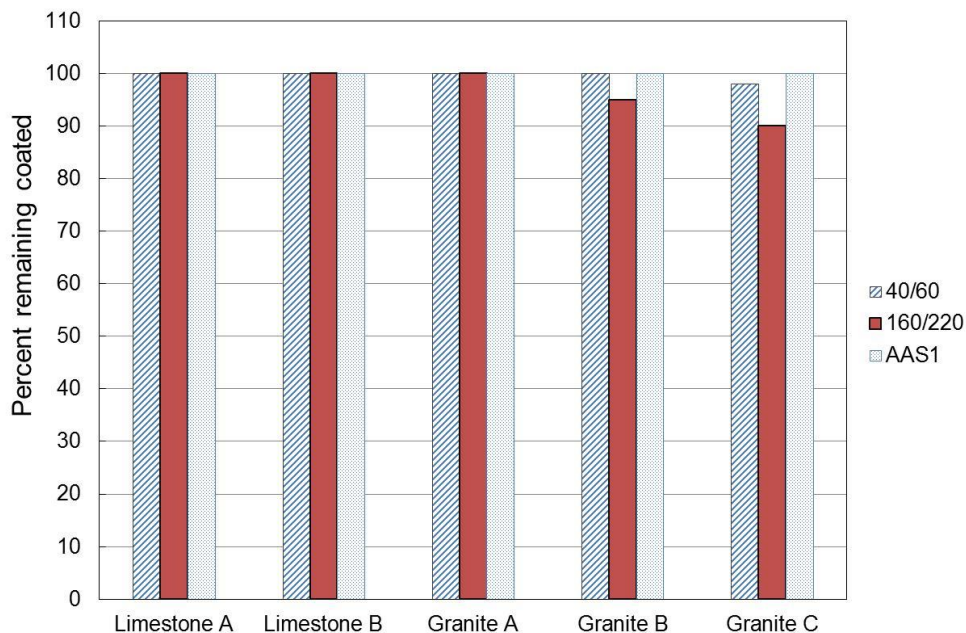


Figure 4. Percent aggregate coating after static immersion test

The results suggest that most of the aggregate/binder combinations showed similar bonding (greater than 95% of coated aggregates) properties after undergoing the static immersion test. The exception was the combinations of Granite C which showed a 10% striped aggregate result with the 160/220 pen bitumen. Granite B showed a 5% stripping value with the 160/220 pen bitumen. These results are in agreement with previous studies (Vuorinen and Hartikainen, 2001; Liu et al., 2014) that used similar aggregates. Results for the mixtures containing amine-based anti-stripping agents with retained binder greater

666 than 95% appear to be in agreement with previous research (Ahmad 2011). Even though
667 the static immersion test ranked the Granite C - 60/200 pen combination as worst in terms
668 of moisture sensitivity, the test appears not to be sensitive to the different aggregate types
669 as it ranked the remaining aggregates with all the binders, except 160/220 pen, equally.

670

671 **3.2 Rolling bottle test**

672

673 The rolling bottle test (RBT) was conducted in accordance with BS EN 12697-11
674 (Bituminous mixtures - Test methods for hot mix asphalt part 11 - Determination of the
675 affinity between aggregate and bitumen). The RBT is a subjective test in that affinity is
676 expressed by visual estimation of the degree of bitumen coverage on uncompacted
677 bitumen-coated mineral aggregate particles after the influence of mechanical stirring
678 action in the presence of water. To perform the test, dust-free aggregate samples
679 weighing 170 g were dried in an oven at $105\pm 5^{\circ}\text{C}$ overnight to constant mass and then
680 coated with 5.7 g of molten binder. Mixing of the aggregates with binder was conducted
681 at $120\pm 5^{\circ}\text{C}$. The aggregate-binder mixture was then cooled loose at room temperature.
682 The loose mixture was stored at ambient temperature for 12 to 64 hours before testing.
683 Each of the test bottles were filled to about half their volume with deionized water and
684 about 150 g of the loose aggregate-mixture was placed in each bottle. The whole
685 assembly was put in the bottle roller rotating at a speed of 60 rotations per minute for six
686 hours. At the end of the six-hour period, the aggregate particles were emptied from the
687 test bottle into a test bowl which was then filled with fresh, de-ionized water to a level
688 just above the top of the surface of the particles. Subsequently, the test bowl was placed
689 on a white surface. The purpose of adding fresh water was to allow for optimal visual
690 determination of binder coverage on the aggregate particles. At least three replicates of
691 each sample were tested.

692

693 At the end of the test, the degree of bitumen coverage of the aggregate particles was
694 estimated by visual observation and recorded to the nearest 5%. The degree of bitumen
695 coverage was defined as the average proportion of the surface area of the aggregate
696 particles covered with bitumen, expressed as a percentage (equal to 100 minus the
697 percentage of stripping). The procedure (i.e. rotation in the bottle roller and measuring of
698 bitumen coverage) was repeated for three more cycles (24 hours, 48 hours, and 72 hours)
699 with fresh water replacing the fouled water in the test bottle at the end of each cycle and

700 the degree of bitumen coverage being measured. For each rolling time (6, 24, 48, and 72
701 hours), the mean value for each repeat was calculated to the nearest 5% and the results
702 averaged to obtain the average degree of bitumen coverage for a given mixture.

703

704 Mixtures containing the unmodified binders showed higher binder loss than the modified
705 binder containing anti-stripping agent. Binder losses in the mixtures containing the
706 160/220 pen binder were highest for each aggregate type tested (Figure 5). Binder losses
707 in the 40/60 pen mixtures were just slightly less than 160/220 pen binder although both
708 were higher than the mixtures containing anti-stripping agent for all of the aggregates
709 considered.

710

711

712

713

714

715

716

717

718

719

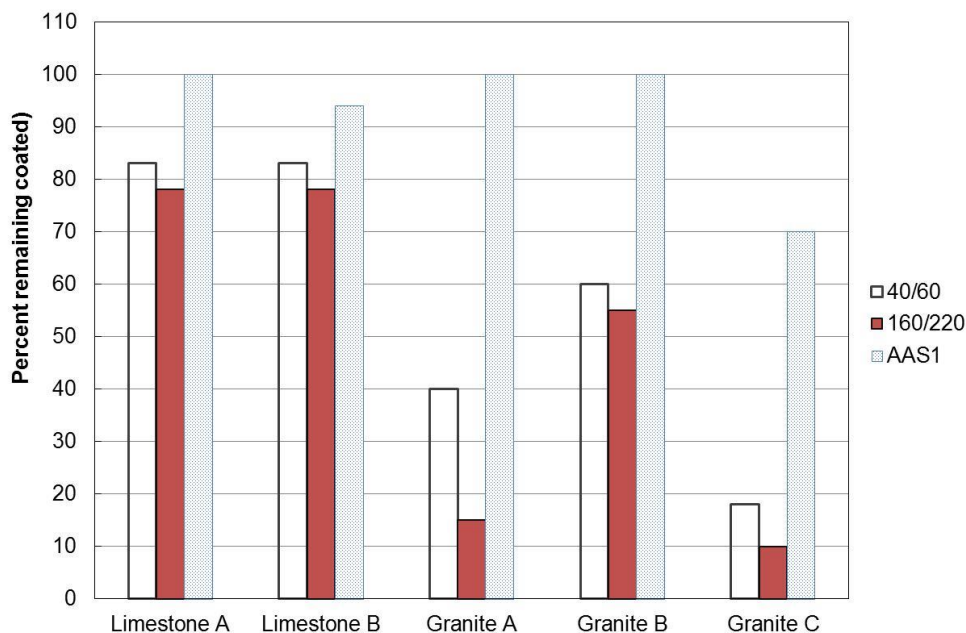
720

721

722

723

724



725 Figure 5. Percent aggregate coating after 72 hours of RBT

726

727 The results show that the rolling bottle test is sensitive to changes in aggregate and binder
728 property including binder modification. Compared to the static immersion test, the rolling
729 bottle appears more discriminatory as it was able to show small differences in moisture
730 susceptibility in the good performing limestone aggregates. For example, ranking in this
731 case was (in increasing order of resistance) 160/220 pen, 40/60 pen and amine-based anti-
732 stripping agent, which was to be expected.

733

734 Compared to the static immersion test, the sensitivity of the rolling bottle test was higher.
735 Figure 6 shows the binder loss versus conditioning time obtained for mixtures containing
736 40/60 pen binder that illustrates the sensitivity of the rolling bottle test to different
737 aggregate types. The limestone aggregates (Limestone A and B) perform better than the
738 granite aggregates (Granite A, B and C). The results showing Granite C as the worst
739 performing aggregate again are as expected based on field performance.

740

741 From the curves in Figure 6, it could be seen that the percentages of bitumen coverage
742 decreased slowly with testing time for limestone, while on the contrary, percentages
743 for granite reduce sharply during the test period. For instance, during the first six
744 hours, Limestone B showed only a 2% binder loss while Granite C showed about 20%
745 loss. In addition, the percentage of binder loss for Granite C at 6 hours is equal to that
746 for the limestone aggregates at 72 hours. Among the granite aggregates, Granite B
747 showed the best bonding properties as illustrated by the 10%, 15%, 30%, 40% of
748 binder loss for 6, 24, 48 and 72 hours, respectively. Although the total loss of binder
749 for Granite A was more than Granite B, these two aggregate had almost the same
750 percentage of binder loss after the first 24 hours. Similar results were obtained for the
751 softer 160/220 pen binder.

752

753

754

755

756

757

758

759

760

761

762

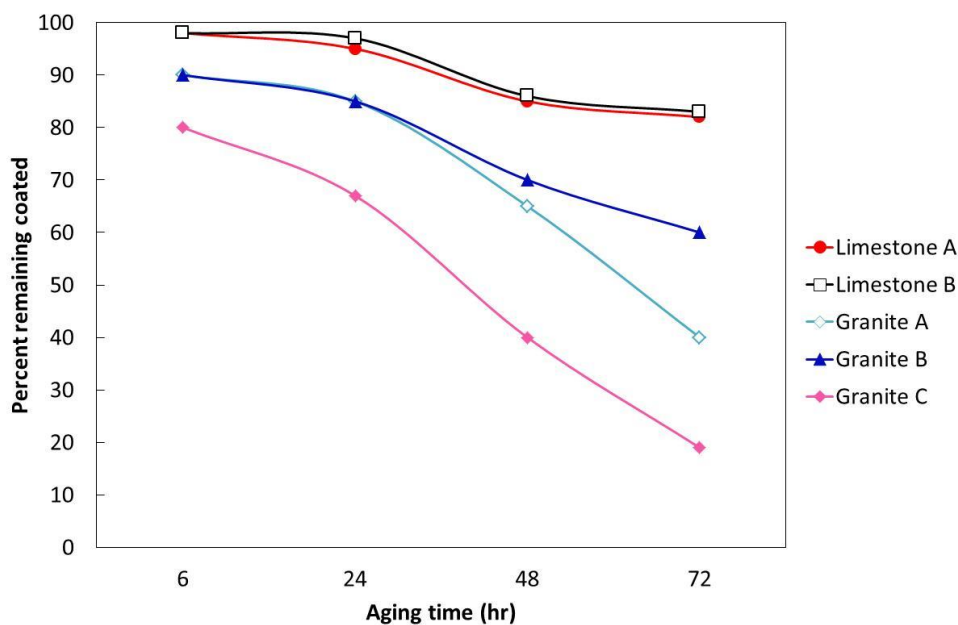
763

764

765

766 Figure 6. Kinetics of bitumen coverage of aggregates during RBT

767



768 **3.3 Boiling Water Test**

769

770 The boiling water test was performed in accordance with ASTM D3625 - 96(2005)
771 (Standard Practice for Effect of Water on Bituminous-Coated Aggregate Using Boiling
772 Water). Compared with the static immersion and rolling bottle tests, the boiling water
773 test is a quicker approach to evaluate the moisture sensitivity of the bitumen and
774 aggregate combination since it only takes about 60 minutes to condition the sample
775 compared with more than 72 hours for the rolling bottle test or 16 to 18 hours in the case
776 of the static immersion test. Like the static immersion test, the boiling water test cannot
777 be used as a measure of field performance because such correlations have not been
778 established. At least three replicates of each sample were tested.

779

780 To perform the test, 600 g of clean oven-dried aggregates were fully coated with 30 g of
781 molten binder. About 300 g each of the aggregate-bitumen mixture was submerged under
782 boiling water in a glass beaker and the mixture boiled for 10 minutes. The percentage of
783 the total visible area of the aggregate that retained its original coating of bitumen was
784 used as an estimate of moisture damage. Only two binders (40/60 pen and 160/220 pen)
785 were evaluated using the boiling water test.

786

787

788

789

790

791

792

793

794

795

796

797

798

799

800

801

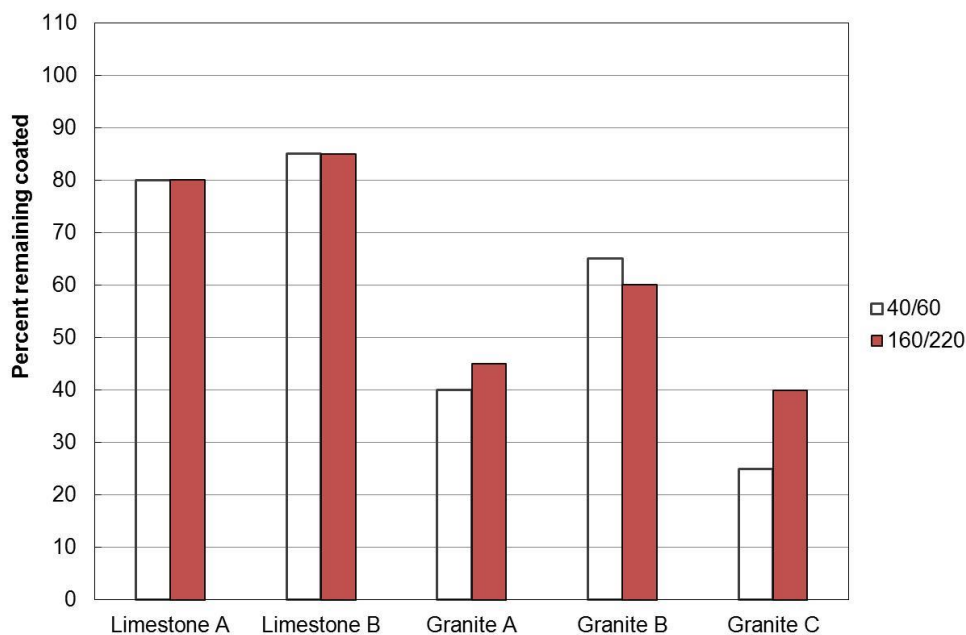


Figure 7. BWT results for different aggregate-bitumen systems

802 The results are shown in Figure 7 where Granite C again exhibited the worst bonding
803 properties. Considering the limestone aggregates, the performance of Limestone A and B
804 was similar for both 40/60 pen and 160/220 pen binder. In terms of the granite
805 aggregates, the 160/220 pen binder showed better bond performance than the 40/60 pen
806 binder except for Granite A.

807

808 **3.4 Total Water Immersion Test**

809

810 The total water immersion test (TWIT) was performed in the laboratory to compare the
811 performance of bitumen doped with an adhesion agent against the non-doped bitumen.
812 This is necessary to check each aggregate with non-doped and doped bitumen to assess
813 the effectiveness of the additive or whether the aggregate needs additive in the binder to
814 provide proper adhesion. Three replicates of each sample were tested.

815

816 The test assesses the average percentage of binder coverage after immersion in 40°C
817 water after 3 hours of soaking. The test is an improvement on the static immersion test. It
818 uses water at 40°C rather than room temperature (25°C) used in the static immersion test
819 to provide a better result. Again only two binders (40/60 pen and 160/220 pen) were
820 evaluated using the total water immersion test.

821

822

823

824

825

826

827

828

829

830

831

832

833

834

835

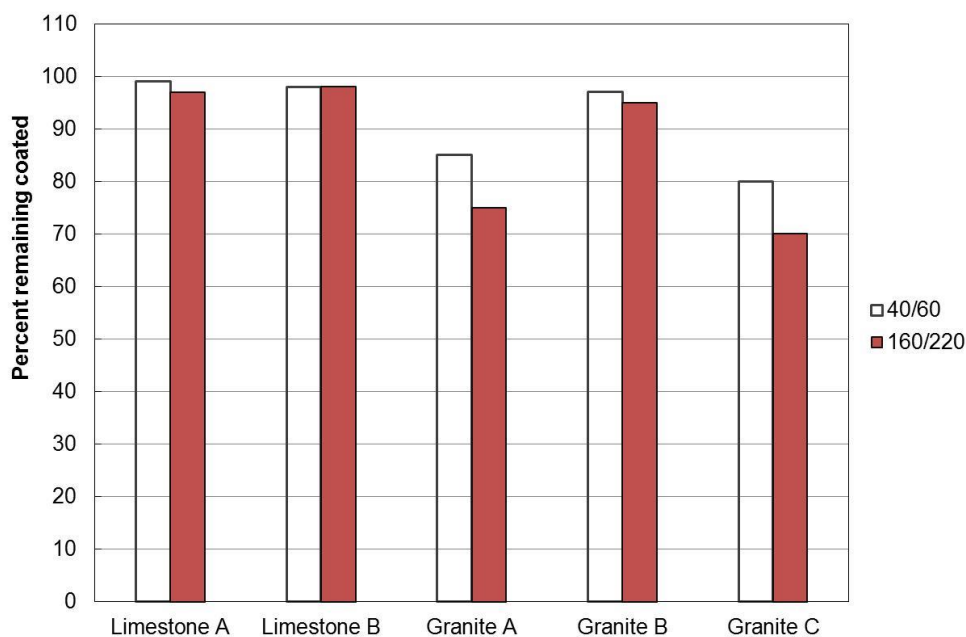


Figure 8. TWIT results for different aggregate-bitumen systems

836 Figure 8 shows the average percentage of binder coverage after immersion in 40°C water
837 for 3 hours obtained during the total water immersion test. From Figure 8, it can be seen
838 that the limestone aggregates had very little binder loss compared with the granite
839 aggregates. The percentages of binder loss for limestone were all less than 5% for the two
840 binder types. The results for the granite aggregates showed higher percentages of binder
841 loss. As in the previous stripping tests, Granite C showed the worst performance with
842 20% and 30% binder loss, for 40/60 pen and 160/220 pen, respectively.

843

844 **4. Asphalt mixture moisture conditioning using the SATS procedure**

845

846 SATS is the first procedure of its kind that combines both ageing and water damage
847 mechanisms (subjected to asphalt pavements in service) within a single laboratory test
848 protocol. The procedure has been found to successfully reproduce the moisture
849 damage observed in asphalt materials in the field (Collop et al. 2004a) as well as
850 distinguish between poor performing material and alternative asphalt mixtures
851 incorporating aggregate with good durability track records (Choi et al, 2002, Airey et
852 al. 2003, Collop et al. 2004b and Choi, 2005). The results obtained from the SATS
853 moisture conditioning procedure tend to rank asphalt mixtures in terms of moisture
854 sensitivity in the same order as the AASHTO T283 procedure (Anon, 2000), although
855 the relative performance of a mixture containing a moisture sensitive aggregate is
856 usually significantly lower in the SATS test (Airey et al., 2005).

857

858 The standard SATS procedure involves conditioning five pre-saturated specimens
859 simultaneously in a pressure vessel under 0.5 MPa air pressure at a temperature of
860 85°C for a period of 24 hours. This conditioning is followed by a cooling period of 24
861 hours before the air pressure is released and the vessel opened to remove the
862 specimens for stiffness testing (Grenfell et al., 2012). The pressure vessel used can
863 hold five nominally identical specimens (100 mm in diameter and 60 mm in
864 thickness) in a custom-made specimen tray. The dimensions and specifications of the
865 SATS testing equipment, including the size and spacing of the holes in the perforated
866 trays are detailed in Clause 953 of Volume 1 of the UK Manual of Contract
867 Documents for Highway Works, 2004 (MCHW, 2004). The conditions used with the
868 SATS procedure were selected in order to reproduce in the laboratory, the field
869 observed moisture damage as demonstrated by a decrease in stiffness modulus for

870 particular asphalt mixtures as detailed by Airey *et al.* (2005). The key features of the
871 conditioning procedure can be summarised as follows:

872

- 873 • A well-insulated, heated pressure vessel capable of holding five compacted
874 asphalt specimens (100 mm diameter × 60 mm height).
- 875 • Conditioning set-up allowing simultaneous pressure and temperature control.
- 876 • Asphalt specimens, which have been pre-saturated with water (under vacuum),
877 located on a purpose-built tray.
- 878 • A pre-determined quantity of water placed in the vessel so that the bottom
879 specimen is fully immersed during the conditioning procedure.
- 880 • Simultaneous conditioning of five specimens under 0.5 MPa air pressure at a
881 temperature of 85°C for 24 hours, followed by a cooling-down period of 24
882 hours before the pressure is released and the vessel opened to remove the
883 specimens for stiffness testing.

884

885 The ten steps of the SATS conditioning and test procedure as specified in Clause 953
886 are as follows:

887

- 888 1. The unconditioned (initial) indirect tensile stiffness modulus of each asphalt
889 mixture specimen is determined at 20°C using the Nottingham Asphalt Tester
890 (NAT) (Cooper and Brown, 1989) in accordance with BS EN 12697-26 Annex
891 C (124msec rise time, 5µm peak transient horizontal diametral deformation)
892 (BSI 2004a).
- 893 2. The dry mass of each specimen is determined by weighing.
- 894 3. The specimens are subsequently immersed in distilled water at 20°C and
895 saturated using a residual pressure of 35 kPa (i.e. 65 kPa below atmospheric
896 pressure) for 30 minutes.
- 897 4. The wet mass of each specimen is determined by weighing, and the percentage
898 saturation of each specimen calculated, referred to as ‘initial saturation’.
- 899 5. The SATS pressure vessel is partly filled with a pre-determined amount of
900 distilled water (final water level between the bottom, submerged specimen and
901 the above ‘dry’ (pre-saturated specimen)). The pressure vessel and water are

902 maintained at the target temperature of 85°C for at least 2 hours prior to
903 introducing the specimens.

904 6. The saturated asphalt specimens are then placed into the pressure vessel, the
905 vessel is sealed and the air pressure is gradually raised to 0.5 MPa.

906 7. The specimens are maintained at the testing conditions, i.e. 0.5 MPa and 85°C
907 for 24 hours.

908 8. After 24 hours, the target vessel temperature is reduced to 30°C and the vessel
909 is left for 24 hours to cool. When the pressure vessel display temperature has
910 reduced to 30°C (after the 24 hour cooling period) the air pressure is gradually
911 released. When the vessel has achieved atmospheric pressure, it is opened and
912 the specimens removed. Each specimen is then surface dried and weighed in
913 air. The percentage saturation calculated at this stage is referred to as the
914 ‘retained saturation’ (BSI 2003a, BSI 2004b, BSI 2009).

915 9. The specimens are finally brought back to 20°C and the conditioned (final)
916 stiffness modulus determined using a NAT.

917 10. The ratio of the final stiffness modulus / initial stiffness modulus can thus be
918 calculated, and is referred to as the ‘retained stiffness modulus’.

919

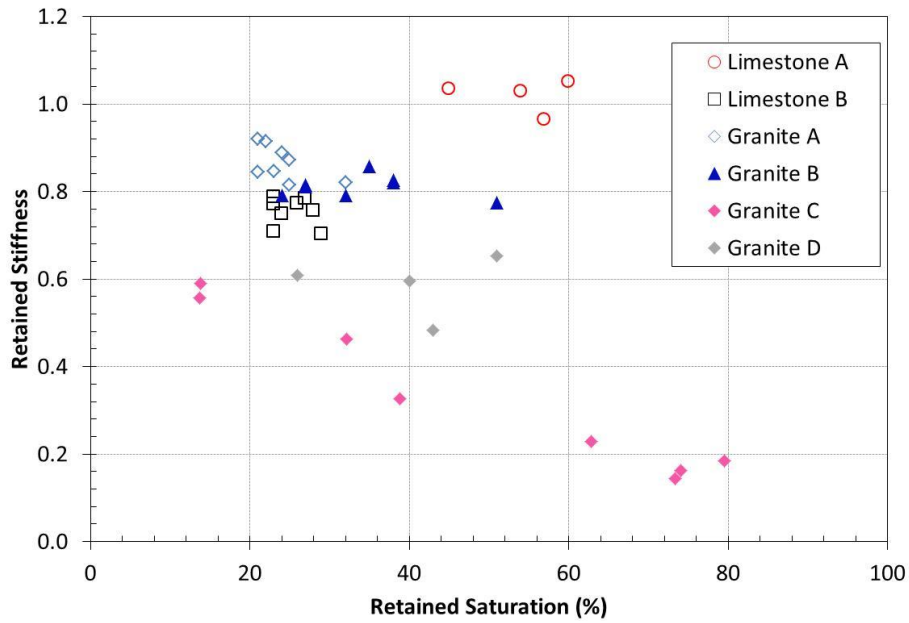
920 During the test there is a continuous cycling of moisture within the pressure vessel,
921 which causes condensation on the underside of the top lid and ‘dripping’ onto the top
922 specimen. There is then a cascading effect where progressively smaller amounts of
923 water ‘drip’ onto the specimens below, resulting in a decrease in retained saturation
924 level for specimens that are located lower down inside the pressure vessel.

925

926 Ten combinations of the five aggregates (two limestones and three granites) and two
927 bitumens (10/20 and 40/60 penetration grades) were included in the study. A standard
928 continuously graded 0/32 mm (28 mm) dense bitumen macadam (DBM) base material
929 was used with the five aggregate types. A target binder content of 4% by total mixture
930 mass was selected for all the asphalt mixtures and roller compacted slabs (305 mm x
931 305 mm x 100 mm) were manufactured and finally cored and trimmed to produce 100
932 mm diameter by 60 mm high specimens with a target air voids content of between 8
933 and 10% (typical of field cores). Only cores that achieved this target were selected for
934 the SATS test.

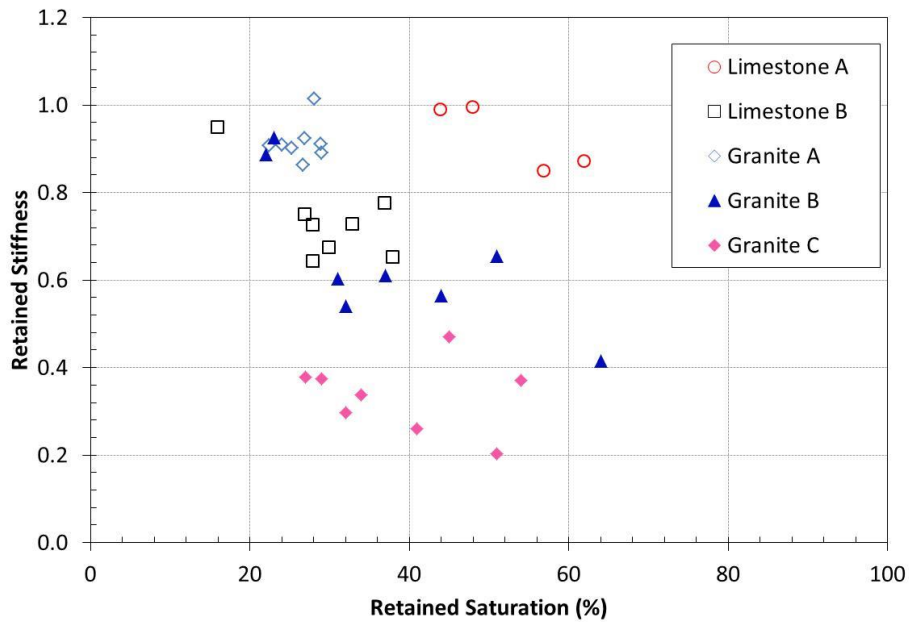
935

936
937
938
939
940
941
942
943
944
945
946
947



948 Figure 9. SATS results for asphalt mixtures with 10/20 pen bitumen
949

950
951
952
953
954
955
956
957
958
959
960
961



962 Figure 10. SATS results for asphalt mixtures with 40/60 pen bitumen
963

964 Results from the SATS tests using the 10/20 and 40/60 pen bitumen can be seen in
965 Figures 9 and 10. Both sets of results demonstrate the high moisture resistance of the
966 mixtures made with limestone aggregate. It can be seen that the retained stiffness for
967 the limestone mixtures is in excess of 0.6, whereas the results for Granite C mixtures
968 are generally in the range between 0.2 and 0.5. The results for Granite A and B
969 mixtures for asphalt mixtures using both the 10/20 and 40/60 pen bitumen tend to be

970 superior to those seen for Granite C. The results for the 10/20 pen bitumen (Figure 9)
 971 even show the performance for Granite A and B to be comparable to those of the two
 972 limestone mixtures although the saturation levels for the Granite A mixtures are
 973 relatively low. Granite A also has a similar performance to the two limestone
 974 aggregates for the softer 40/60 pen bitumen asphalt mixtures in Figure 10, although
 975 once again the saturation levels are considerably lower than those experienced for the
 976 other four mixtures.

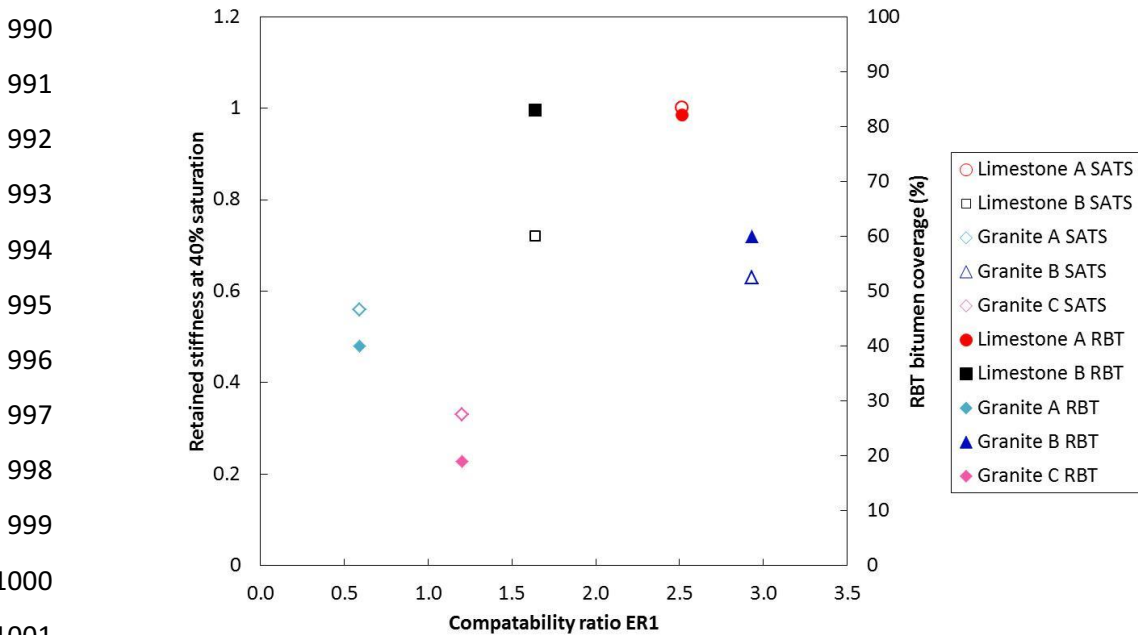
977

978 **5. Relation between intrinsic adhesion, stripping and moisture damage**

979

980 As previously indicated, the key objective of this study was to determine if the
 981 moisture sensitivity assessment parameters for different bitumen-aggregate
 982 combinations obtained by using surface energy parameters of the individual materials
 983 can identify ‘good’ and ‘poor’ performing asphalt mixtures and to determine how the
 984 surface energy-based prediction compare with two standard types of test, for example
 985 the RBT (stripping) and SATS (asphalt mixture) procedures. Previous studies have
 986 shown that both the BWT and TWIT empirical tests have poor correlation with
 987 surface energy parameters and SATS results due to the insufficient sensitivity of these
 988 two aggregate-bitumen stripping tests (Liu et al., 2014).

989



1000

1001

1002

1003 Figure 11. Relationship between SATS, RBT and ER₁

1004 Figures 11 to 14 show plots depicting the relationships between SATS retained
 1005 stiffness (at 40% moisture saturation), the RBT percent bitumen coverage (after 72
 1006 hours) and the four bond energy parameters (ER₁, ER₂, ER₃ and ER₄) for all mixtures
 1007 produced with the 40/60 pen bitumen. It is worth reiterating that the energy ratios
 1008 used in Figures 11 to 14 for Limestone B (black squares) are conservative values and
 1009 are expected to be higher (located further to the right in the graphs) as discussed in
 1010 Section 2.4. The SATS results at 40% moisture saturation have been determined by
 1011 fitting a linear regression line to the data in Figure 10 and calculating the resulting
 1012 retained stiffness at 40% moisture saturation (Grenfell et al., 2012).

1013

1014 In all cases a higher value of the parameter suggests better resistance to moisture
 1015 damage. On this basis, aggregate-bitumen combinations plotting near the upper right
 1016 hand side of the plot (equivalent to higher values of energy ratio, RBT coverage
 1017 and/or SATS retained stiffness) are expected to be more moisture resistant than
 1018 mixtures plotting in the lower left hand side. The results show in general that for all
 1019 four plots the limestone mixtures tend to perform better than the granite mixtures with
 1020 results in the upper right hand quadrant. The order of the two limestones does
 1021 however change once the SSA of the two aggregates is included in the energy ratio
 1022 (ER₃ and ER₄ in Figures 13 and 14) compared to ER₁ and ER₂ in Figures 11 and 12.

1023

1024

1025

1026

1027

1028

1029

1030

1031

1032

1033

1034

1035

1036

1037

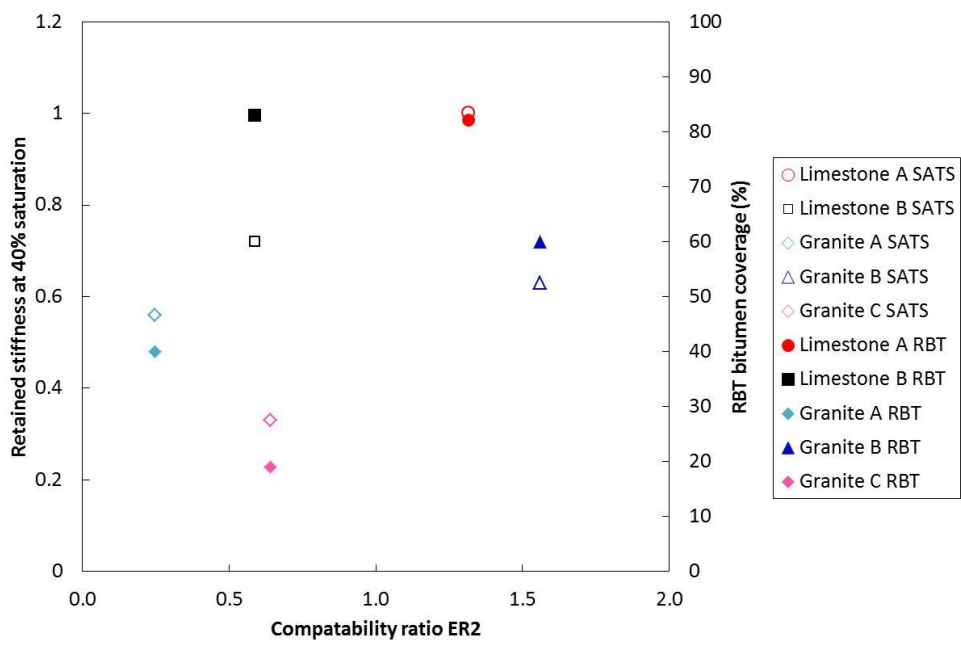
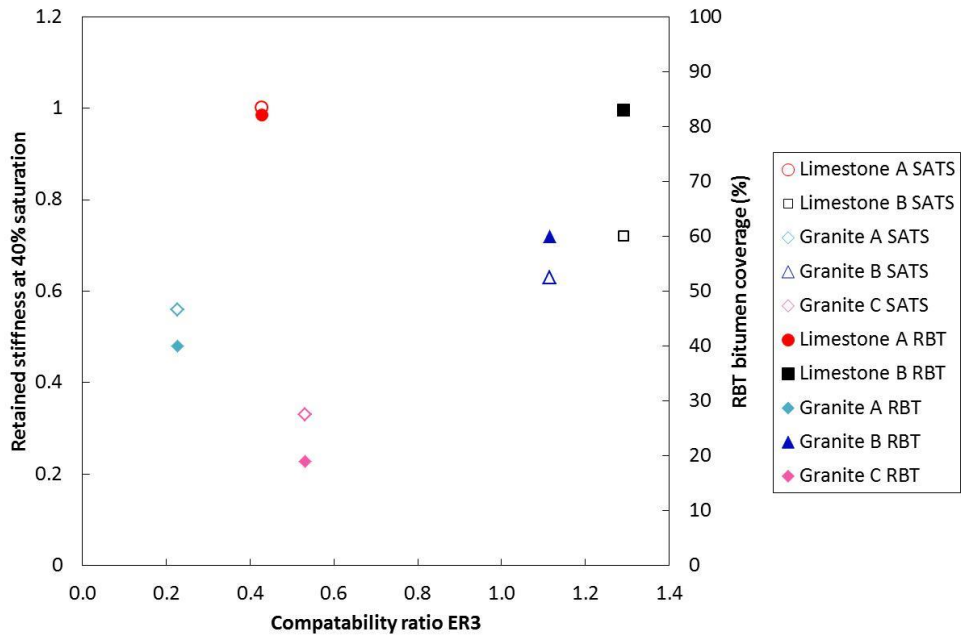


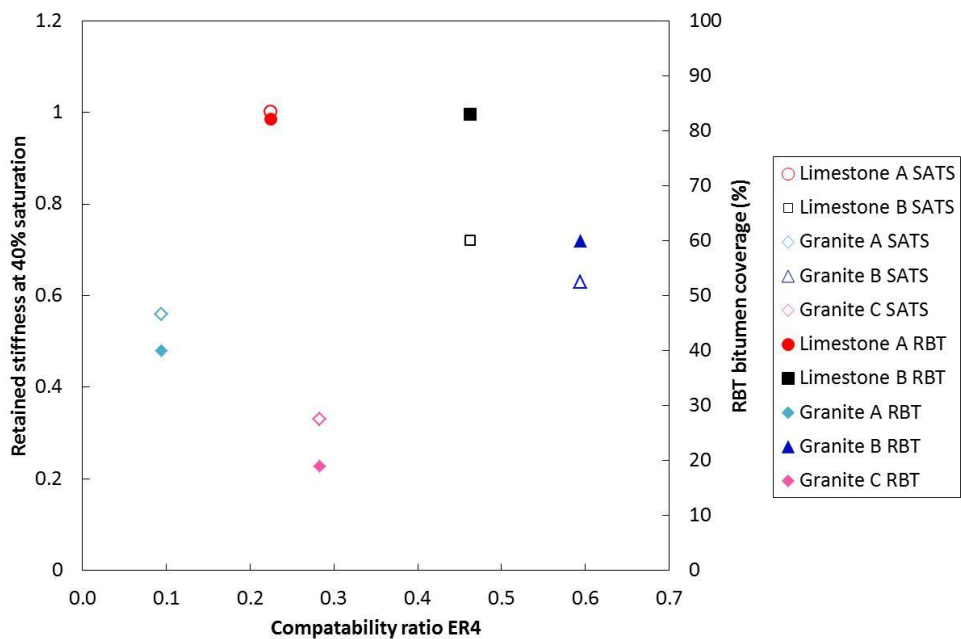
Figure 12. Relationship between SATS, RBT and ER₂

1038
 1039
 1040
 1041
 1042
 1043
 1044
 1045
 1046
 1047
 1048
 1049
 1050



1051 Figure 13. Relationship between SATS, RBT and ER₃

1052
 1053
 1054
 1055
 1056
 1057
 1058
 1059
 1060
 1061
 1062
 1063
 1064
 1065



1066 Figure 14. Relationship between SATS, RBT and ER₄

1067
 1068 In terms of the three granite aggregates, there is a far degree of scatter with Granite A
 1069 tending to have the lowest values (low predicted moisture performance) based on
 1070 intrinsic adhesion and energy ratios but intermediate actual performance in terms of
 1071 RBT and SATS). The results for Granite B tend to sit in the upper right hand quadrant

1072 and demonstrate comparable moisture damage performance to that seen for the two
1073 limestone aggregate mixtures. However, the results for Granite C tend to consistently
1074 fall in the lower left hand quadrant.

1075

1076 The 'good' performance of most of the limestone mixtures observed in this study can
1077 be attributed to their physico-chemical and mineralogical characteristics, while the
1078 range of performance found for the granite aggregates reflects the mineralogical
1079 complexity of these aggregate types.

1080

1081 **6. Conclusions**

1082

1083 This paper presents results from stripping tests, such as the RBT, and asphalt mixture
1084 moisture conditioning procedures, such as SATS, in an attempt to better understand
1085 the underlying processes and mechanisms of moisture damage with the help of
1086 surface energy measurements on the constituent materials (bitumen and aggregates)
1087 and aggregate mineralogy from MLA measurements. The following conclusions were
1088 reached based on the results presented in the paper.

1089

- 1090 • Surface energy parameters obtained from the DCA testing suggests cohesive
1091 strength varies with bitumen grade. Surface energy of the soft bitumen (70/100
1092 pen) was approximately 60% that of the stiffer bitumens (10/20 and 40/60
1093 pen).
- 1094 • The adhesive bond strengths for both the dry and the wet conditions were used
1095 to compute four compatibility ratios using the surface energy parameters
1096 obtained for the bitumen and aggregates. Higher magnitudes of the ratios
1097 suggest better resistance to moisture damage. The results show that for a given
1098 aggregate, moisture resistance of stiffer binders is higher than softer binders.
1099 The results also show that for a given bitumen grade, and for the aggregates
1100 considered in this study, the limestone aggregate mixtures should exhibit
1101 higher resistance (higher ratios) to moisture damage.
- 1102 • The four aggregate-bitumen bond energy parameters (ER_1 , ER_2 , ER_3 and ER_4)
1103 can be used to predict moisture sensitivity of asphalt mixtures using threshold
1104 values (0.75 for ER_1 , 0.50 for ER_2 , 0.50 for ER_3 and 0.35 for ER_4) defined to
1105 separate 'good' from 'poor' moisture damage performing aggregate-bitumen

1106 combinations. Most of the aggregates that were identified as ‘poor’ aggregates
1107 in this study have also been found to perform poorly in previous studies. In
1108 general Limestone A and B can be defined as ‘good’ while Granite C can be
1109 defined as ‘poor’. The remaining two granite aggregates (Granite A and B) can
1110 be considered to have intermediate moisture damage performance.

- 1111 • The bond energy parameters (ER_1 , ER_2 , ER_3 and ER_4) have been developed
1112 for aggregate-binder systems that demonstrate a negative value for the work of
1113 adhesion under ‘wet’ conditions (W_{BWA}^a) and are therefore are not applicable
1114 for the systems containing Limestone B which produced positive values of
1115 W_{BWA}^a . It is therefore important to consider the energy ratio results for
1116 Limestone B as conservative values.
- 1117 • Compared to the ER_1 and ER_2 parameters, the results for ER_3 and ER_4 showed
1118 the significant influence of SSA on the selection of ‘good’ versus ‘poor’
1119 moisture damage performing aggregate-bitumen combinations. Because of the
1120 apparent large influence of SSA on moisture sensitivity of asphalt mixtures
1121 shown in this study, the bond parameters ER_3 and ER_4 appear to be more
1122 suitable indices for determining the performance of the different aggregate-
1123 bitumen combinations with a clear distinction in terms of ‘good’ and ‘poor’
1124 aggregates.
- 1125 • Results from the RBT showed that the percentage of bitumen coverage (a
1126 measure of adhesiveness) varies depending on aggregate type. About 90% of
1127 the limestone aggregates remained coated with bitumen at the end of the
1128 rolling bottle test compared with only 20% for one of the granite aggregate.
1129 This suggests that in the presence of moisture, limestone aggregates will
1130 generally tend to maintain a better adhesive bond with bitumen than granite
1131 aggregates although this will depend on the specific mineralogy of the granite.
- 1132 • Moisture damage factors (moisture factors) obtained from the SATS tests for
1133 limestone aggregate asphalt mixtures were comparatively higher than that for
1134 certain granite mixtures. Higher moisture factors indicate better moisture
1135 resistance.
- 1136 • Mineralogical testing of the aggregates, using MLA, showed considerable
1137 differences not only between limestone and granite but also between different
1138 granites. Differences in moisture sensitivity of the mixtures observed in this

1139 study for the different aggregates can be attributed in part to aggregate
1140 mineralogy.

1141 • It is concluded that moisture resistance of asphalt mixtures are influenced by
1142 the mineralogical composition of the aggregates as well as the adhesive bond
1143 between the aggregate and bitumen in the presence of moisture. Both the RBT
1144 and SATS are useful in evaluating moisture damage in asphalt mixtures as the
1145 ranking obtained in these empirical tests are similar to surface energy and
1146 mineralogical characteristics of the asphalt mixtures.

1147 • The surface energy testing protocols and adhesive bond strength calculations
1148 can be used to compliment available asphalt mixture design methods by
1149 identifying compatible bitumen-aggregate combinations. Surface energy
1150 properties of the materials combined with the parameters obtained by
1151 conventional moisture sensitivity assessment techniques can also contribute
1152 towards the development of a material screening protocol. This protocol can
1153 then be used for determining the best combinations of bitumen and aggregates
1154 for the local road material providing better bitumen-aggregate adhesion and
1155 less susceptibility to moisture damage/stripping.

1156

1157 **References**

1158

1159 Abo-Qudais S, Al-Shweily H. Effect of aggregate properties on asphalt mixtures
1160 stripping and creep behaviour. *Constr Build Mater* 2007;21: 1886–98.

1161 Ahmad, N. Asphalt Mixture Moisture Sensitivity Evaluation Using Surface Energy
1162 Parameters. *PhD Dissertation*. University of Nottingham, Nottingham, 2011.

1163 Airey, G.D., Masad, E.A., Bhasin, A., Caro, S. and Little, D.N. (2007) Asphalt
1164 Mixture Moisture Damage Assessment Combined with Surface Energy
1165 Characterization. *Proceedings of the International Conference on Advanced
1166 Characterisation of Pavement and Soil Engineering Materials*, Vol. 1, 739-
1167 748, Athens.

1168 Airey, G.D., and Choi, Y.K., (2002) State of the Art Report on Moisture Sensitivity
1169 Test Methods for Bituminous Pavement Materials. *Road Materials and
1170 Pavement Design*. Vol. 3, No. 4, 355-372.

1171 Airey, G.D., Choi, Y., Collop, A.C., Moore, A.J.V. and Elliott, R.C., (2005)
1172 Combined laboratory ageing / moisture sensitivity assessment of high modulus
1173 base asphalt mixtures. *Proceedings of the Association of Asphalt Paving*
1174 *Technologists*, Vol. 74, 307-346.

1175 Airey, G.D., Choi, Y., Collop, A.C. and Elliott, R.C., (2003) Development of an
1176 accelerated durability assessment procedure for high modulus base (HMB)
1177 materials. *6th International RILEM Symposium on Performance Testing and*
1178 *Evaluation of Bituminous Materials*, PTEBM'03, Zurich, Switzerland.

1179 Airey, G.D., Collop, A.C., Zoorob, S.E. and Elliott, R.C., (2008) The influence of
1180 aggregate, filler and bitumen on asphalt mixture moisture damage.
1181 *Construction and Building Materials*. Vol. 22, 2015–2024.

1182 Annual Local Authority Road Maintenance (Alarm) Survey, Asphalt Industry
1183 Alliance, (2010). www.asphaltindustryalliance.com/alarm.asp.

1184 Anon, (2000) Resistance of compacted bituminous mixtures to moisture induced
1185 damage. AASHTO T283-99, American Association of State Highways and
1186 Transportation Officials, USA.

1187 Audit Scotland, Maintaining Scotland's roads: a follow-up report, (2010). [www.audit-](http://www.audit-scotland.gov.uk/docs/central/2010/nr_110216_road_maintenance.pdf)
1188 [scotland.gov.uk/docs/central/2010/nr_110216_road_maintenance.pdf](http://www.audit-scotland.gov.uk/docs/central/2010/nr_110216_road_maintenance.pdf).

1189 Bhasin, A. (2006) Development of Methods to Quantify Bitumen-Aggregate
1190 Adhesion and Loss of Adhesion due to Water: PhD dissertation, Texas A&M
1191 University, USA.

1192 Bhasin, A., Masad, E., Little, D., and Lytton, R., (2006) Limits on Adhesive Bond
1193 Energy for Improved Resistance of Hot-Mix Asphalt to Moisture Damage.
1194 *Transportation research record: Journal of the Transportation Research*
1195 *Board*, No. 1970, Washington D.C., 3-13.

1196 British Standards Institution, 2003a. Bituminous mixtures – Test methods for hot mix
1197 asphalt – Part 6: Determination of bulk density of bituminous specimens, BS
1198 EN 12697-6: London.

1199 British Standards Institution, 2003b. Bituminous mixtures – Test methods for hot mix
1200 asphalt – Part 8: Determination of void characteristics of bituminous
1201 specimens, BS EN 12697-8: London.

1202 British Standards Institution, 2004a. Bituminous mixtures – Test methods for hot mix
1203 asphalt – Part 26: Stiffness, BS EN 12697-26: London.

1204 British Standards Institution, 2009. Bituminous mixtures – Test methods for hot mix
1205 asphalt – Part 5: Determination of the maximum density, BS EN 12697-5:
1206 London.

1207 Caro S, Masad E, Bhasin A, Little DN. Moisture susceptibility of asphalt mixtures,
1208 Part 1: mechanisms. *Int J Pavement Eng* 2008;9:81–98.

1209 Caro S, Masad E, Bhasin A, Little DN. Moisture susceptibility of asphalt mixtures,
1210 Part 2: characterisation and modelling. *Int J Pavement Eng* 2008;9:99–114.

1211 Caro S, Masad E, Bhasin AH, Little D. Micromechanical modelling of the influence
1212 of material properties on moisture-induced damage in asphalt mixtures. *Constr*
1213 *Build Mater* 2010;24:1174–92.

1214 Cheng, D. (2002) Surface Free Energy of Asphalt Aggregate System and Performance
1215 Analysis of Asphalt Concrete based on Surface Free Energy: PhD dissertation,
1216 Texas A&M University, USA.

1217 Cheng, D., Little, D.N., Lytton, R.L. and Holste, J.C. (2002a). Surface Energy
1218 Measurement of Asphalt and Its Application to Predicting Fatigue and Healing
1219 in Asphalt Mixtures. *Transportation Research Record: Journal of the*
1220 *Transportation Research Board*, No. 1810, TRB, National Research Council,
1221 Washington, D.C., 44-53.

1222 Cheng, D., Little, D.N., Lytton, R.L., and Holste, J.C., (2002b) Moisture Damage
1223 Evaluation of Asphalt Mixtures by Considering both Moisture Diffusion and
1224 Repeated-Load Conditions. *Transportation Research Record: Journal of the*
1225 *Transportation Research Board*. TRR 1832, 42-49.

1226 Choi, Y.K., Collop, A.C., Airey, G.D., Elliott, R.C., Williams, J. and Heslop, M.W.,
1227 (2002) Assessment of the durability of high modulus base (HMB) materials.
1228 *6th International Conference on the Bearing Capacity of Roads, Railways and*
1229 *Airfields*, Lisbon, Portugal.

1230 Choi, Y.C., (2005) Development of the saturation Ageing Tensile Stiffness (SATS)
1231 Test for High Modulus Base Materials. PhD Thesis, School of Civil
1232 Engineering, University of Nottingham, UK.

1233 Collop, A.C., Choi, Y.K., Airey, G.D. and Elliott, R.C., (2004a) Development of the
1234 saturation ageing tensile stiffness (SATS) test. *Proceedings of the ICE*
1235 *Transport*, 157, 163-171.

1236 Collop, A.C., Choi, Y.K. and Airey, G.D., (2004b) Development of a combined
1237 ageing / moisture sensitivity laboratory test. *Euroasphalt and Eurobitume*
1238 *Congress*, Vienna, Austria.

1239 Cooper, K.E. and Brown, S.F., 1989. Developments of a Simple Apparatus for the
1240 Measurement of the Mechanical Properties of Asphalt Mixes. *Proceedings of*
1241 *the Eurobitume Symposium*, Madrid, 494-498.

1242 Emery, J. and Seddik, H. (1997) Moisture-damage of Asphalt Pavements and
1243 Antistripping Additives: Causes, Identification, Testing and Mitigation.
1244 *Transportation Association of Canada*, Ottawa, Canada.

1245 Erbil, H.Y., (2006) Surface Chemistry of Solid and Liquid Interfaces, Blackwell
1246 Publishing Ltd.

1247 Fowkes, F.M. (1962) Determination of Interfacial Tensions, Contact Angles, and
1248 Dispersion Forces in Surfaces by Assuming Additivity of Intermolecular
1249 Interactions in Surfaces, *Journal of Physical Chemistry*, Vol. 66, 382-382.

1250 Gilmore DW, Darland Jr JB, Girdler LM, Wilson DW, Scherocaman JA. Changes in
1251 asphalt concrete durability resulting from exposure to multiple cycles of
1252 freezing and thawing. *ASTM Spec Tech Publ* 1985;899:73–88.

1253 Good, R.J. and C.J. van Oss. (1991) The Modern Theory of Contact Angles and the
1254 Hydrogen Bond Components of Surface Energies, *Modern Approach to*
1255 *Wettability: Theory and Application*. Plenum Press, New York.

1256 Good, R.J. (1992) Contact Angle, Wetting, and Adhesion: A Critical Review, *Journal*
1257 *of Adhesion Science and Technology*, Vol. 6, 1269-1302.

1258 Grenfell, J., Ahmad, N. Airey, G., Collop, A. and Elliott, R. (2012) Optimising the
1259 moisture durability SATS conditioning parameters for universal asphalt
1260 mixture application, *International Journal of Pavement Engineering*. Vol. 13,
1261 No. 5, 433-450.

1262 Grenfell, J.R.A., Ahmad, N., Liu, Y., Apeageyi, A.K., Large, D. and Airey, G.D.
1263 ‘Assessing asphalt mixture moisture susceptibility through intrinsic adhesion,
1264 bitumen stripping and mechanical damage.’ *International Journal of Road*
1265 *Materials and Pavement Design*, Vol. 15, No. 1, pp 131-152, 2014.

1266 Horgnies, M., Darque-Ceretti, E., Fezai, H. and Felder, E. (2011) Influence of the
1267 interfacial composition on the adhesion between aggregates and bitumen:
1268 Investigations by EDX, XPS and peel tests, *International Journal of Adhesion*
1269 *and Adhesives*. Vol. 31, Issue 5, 238-247.

1270 Huang S, Robertson RE, Branthaver JF, Petersen JC. Impact of lime modifica-
1271 asphalt and freeze–thaw cycling on the asphalt–aggregate interaction and
1272 moisture resistance to moisture damage. *J Mater Civ Eng* 2005;17:711–8.

1273 Kandhal, P.S. (1994) Field and Laboratory Evaluation of Stripping in Asphalt
1274 Pavements: State of the art. *Transportation Research Record: Journal of the*
1275 *Transportation Research Board*. TRR 1454, TRB, Washington, D.C., 36-47.

1276 Kennedy TW, Roberts FL, Lee KW. Evaluation of moisture susceptibility of asphalt
1277 mixtures using the texas freeze–thaw pedestal test. *Proc Assoc Asphalt*
1278 *Pavement Technol* 1982;51:327–41.

1279 Kennedy TW, Roberts FL, Lee KW. Evaluation of moisture effects on asphalt
1280 concrete mixtures. *Transp Res Rec* 1983;911:134–43.

1281 Kennedy TW, Roberts FL, Lee KW. Evaluating moisture susceptibility of asphalt
1282 mixtures using the texas boiling test. *Transp Res Rec* 1984;968: 45–54.

1283 Kutay ME, Aydilek AH, Masad E. Computational and experimental evaluation of
1284 hydraulic conductivity anisotropy in hot-mix asphalt. *Int J Pavement Eng*
1285 2007;8:29–43.

1286 Little, D.N. and Bhasin, A., 2006. Using surface energy measurements to select
1287 materials for asphalt pavement. NCHRP project 9–37, final report.
1288 Washington, DC: Transportation Research Board, National Research Council.

1289 Liu, Y., Apeageyi, A.K., Ahmad, N., Grenfell, J.R.A. and Airey, G.D. ‘Examination
1290 of moisture sensitivity of aggregate-bitumen bonding strength using loose
1291 asphalt mixture and physico-chemical surface energy property tests.’
1292 *International Journal of Pavement Engineering*, Vol. 15, No. 7, pp 657-670,
1293 2014.

1294 Manual Series No. 24 (MS-24), (2007) Moisture Sensitivity: Best Practices to
1295 Minimize Moisture Sensitivity in Asphalt Mixtures, Asphalt Institute, USA.

1296 Masad E, Al-Omari A, Chen HC. Computations of permeability tensor coefficients
1297 and anisotropy of hot mix asphalt based on microstructure simulation of fluid
1298 flow. *Comput Mater Sci* 2007;40:449–59.

1299 MCHW, 2004. Method for the Assessment of Durability of Compacted Asphalt
1300 Mixtures using the Saturation Ageing Tensile Stiffness (SATS) Tests. Manual
1301 of Contract Document for Highways Works: Clause 953, Highways Agency,
1302 UK.

1303 Miller, J.S. and Bellinger, W.Y. (2003) Distress Identification Manual for the Long-
1304 Term Pavement Performance Program. Publication FHWA-RD-03-031.
1305 FHWA, Office of Infrastructure Research and Development, McLean,
1306 Virginia.

1307 Petersen JC, Plancher H, Ensley EK, Venables RL, Miyake G. Chemistry of asphalt-
1308 aggregate interaction: relationship with pavement moisture-damage prediction
1309 test. *Transp Res Rec* 1982;843:95–104.

1310 Shakiba M, Abu Al-Rub RK, Darabi MK, You T, Masad EA, Little DN. Continuum
1311 coupled moisture-mechanical damage model for asphalt concrete. *Transp Res*
1312 *Rec* 2013;2372:72–82.

1313 Shaw, D. J., (1991) Introduction to Colloid and Surface Chemistry, 4th ed. Oxford.
1314 Butterworth-Heinemann.

1315 Sing, K. S. W., (1969) Utilisation of Adsorption Data in the BET Region.
1316 *Proceedings; International Symposium on Surface area Determination,*
1317 Bristol, UK.

1318 Solaimanian, M., J. Harvey, M. Tahmoressi, and V. Tandon. (2003) Test Methods to
1319 Predict Moisture Sensitivity of Hot Mix Asphalt Pavements. *Proceedings*
1320 *National Seminar on Moisture Sensitivity of Asphalt Pavements*, San Diego,
1321 California.

1322 Terrel R.L. and Al-Swailmi S. (1994) Water Sensitivity of Asphalt-Aggregate Mixes:
1323 Test Selection. SHRP-A-403, Strategic Highway Research Program, National
1324 Research Council, Washington, D.C.

1325 Vuorinen, M. and Hartikainen, O.-K., 2001. A new ultrasonic method for measuring
1326 stripping resistance of bitumen on aggregate. *Road Materials and Pavement*
1327 *Design*, 2 (3), 297–309
1328
1329